ELECTROGASDYNAMIC CONTROL OF SEPARATED FLOW, A FEASIBILITY STUDY

John Peter Segen

United States
Naval Postgraduate School

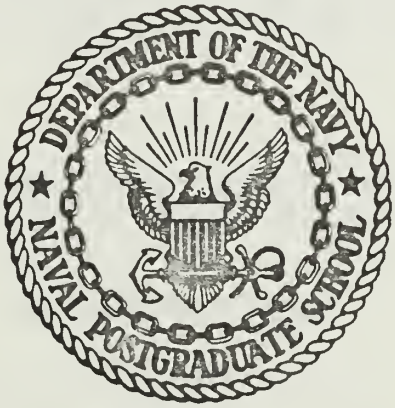

THESIS

Electrogasdynamic Control of Separated Flow,

A Feasibility Study

by

John Peter Segen

June 1970

Electrogasdynamic Control of Separated Flow, A Feasibility Study

by

John Peter Segen
Lieutenant, United States Navy
B.S., University of Colorado,1963

Submitted in partial fulfillment of the
requirements for the degree of

AERONAUTICAL ENGINEER

from the
Naval Postgraduate School
June 1970

ABSTRACT

This investigation proposes to determine if electrogasdynamic interactions are feasible for flow separation control. It is shown theoretically that the electric pressure caused by charged particle movement in an electric field produces a pressure increase that is at the lower limit of values needed for flow separation control. The theoretical possibility is also shown using the Navier-Stokes equations with an electric body-force term included.

An experiment is carried out using charged particle injection and acceleration in a separated region beneath a backward-facing step. The experimental results are inconclusive. Recommendations are given to improve the experiment.

TABLE OF CONTENTS

LIST OF TABLES

LIST OF ILLUSTRATIONS

FIGURE

LIST OF SYMBOLS

A = Cross sectional area of duct

A^* = Area of EGD nozzle exit

a = Cylinder radius

b = Ion or charged particle mobility

c = Chord length

E = Electric field intensity

E_b = Breakdown electric field intensity

E_o = Initial electric field intensity

E_x = Electric field intensity in free stream direction

E_y = Electric field intensity normal to free stream direction

I = Current

I_c = Corona current

I_1 = Collector current

j = Current density

k = Ratio of specific heats

M = Mass flow rate

p = Pressure

p_a = Ambient pressure

p_g = Gage pressure

p_o = Reservoir pressure

r = Distance from origin in polar coordinates

T = Thrust

U_∞ = Free stream velocity

u = Local velocity in axial direction

v_c = Corona potential

v_1 = Collector potential

v = Local velocity in normal direction

W = Electric potential

x = Axial coordinate

y = Normal coordinate

z = Width coordinate

ϱ = Charge density

ϵ = Dialectric constant

μ = Viscosity

ν = Kinematic Viscosity

θ = Angular coordinate

δ = Mass Density

ACKNOWLEDGEMENT

The author wishes to express his appreciation to Professor Oscar Biblarz of the Naval Postgraduate School for all the hours of discussion, instruction and assistance that he gave. Mr. Patrick Hickey deserves acknowledgement for his efforts in behalf of this project and for the high quality of his workmanship. A special thanks is given to the author's family for assuming many of his familial duties and showing an abiding patience as this work progressed.

I. INTRODUCTION

In 1904 Prandtl demonstrated that the extent of a separated flow region about a cylinder could be greatly reduced by suction. Since that time, many boundary layer control devices have been developed and tested. Some of these devices have proved successful, and are currently in use on modern aircraft. The distinguishing characteristics of a successful boundary layer control device are that it be of simple, reliable design and without excessive weight. That is, the total weight of the device, including extra structure required for mounting plus the power generating equipment needed to operate the device, must be less than the lift gained by the use of the device. Applied research in this field proceeds toward the objective of providing the optimum boundary layer control device with regard to benefits obtained, whether it be increased lift or decreased drag, at a minimum weight. With this thought in mind, all practical methods of controlling a boundary layer must be studied. One method that seems possible but needs more study to determine its feasibility is the use of accelerated charged particles as a means of imparting momentum to the stagnant region of a separated flow.

It is not meant to imply that this means of boundary layer control is a completely new idea. The earliest work found, not necessarily the earliest published, in a related area was a master's thesis by Shaar (Ref. 10) in 1947. In this work Shaar shows that the injection of a large number of positive ions into the boundary layer of a diffuser, the walls of which are maintained at floating potential, causes a reduction in height of the boundary layer at the exit. In 1969, Cheng

(Ref. 5) discussed the possibility of reducing separation on an airfoil by using an electric discharge. In this article he states that the pressure gradient in a separated turbulent boundary layer is approximately 10 dynes per cubic centimeter, and that if a corona discharge could exert a pressure of 1000 dynes per square centimeter on the flow the boundary layer would remain attached for about one additional meter downstream. Stuetzer (Ref. 12), in an undated paper, shows a remarkable reduction of the separation on a cylinder and a hydrofoil, which are kept at floating potential, in a flow of kerosene into which ions were injected. Stuetzer also makes use of electric pressure in determining when modifications to the separation pattern can be expected. He uses the ratio of electric pressure to the change in hydrostatic pressure to describe the relative influence of the injected charge, but states that experimental information needed to generalize this parameter to flows other than kerosene are not available.

The idea of viscously coupling particles, of optimal size and charge, has been studied in connection with electrogasdynamic generators (Ref. 7) but it has not been used to control airflows at atmospheric pressure. This project proposes to apply this idea to a subsonic separated airflow. In doing so it specifically endeavors to answer the question: What possibility exists to reduce the extent of separation on an airfoil by adding momentum to the separated region by viscous interaction between electrically accelerated, charged particles and the neutral particles in the separated region?

II. THEORETICAL FEASIBILITY

In recent years much research has been done in the field of electrogasdynamic (EGD) generators. The objective of this work has been to convert the flow energy of a flow into electrical work. This process essentially involves a momentum transfer from the flow particles to the electrically charged particles, which are usually generated by a corona discharge. The momentum gained by the charged particles causes them to move out of the region in which they were produced thereby doing electrical work. They are then collected to close the generator circuit. Although some success has been achieved in these projects the amount of electrical energy made available is generally small (Ref. 4).

A scheme for adding momentum to a separated boundary layer can be devised using a similar principle. Charged particles are injected into the flow in the same manner as an EGD generator and are then accelerated to a velocity higher than the flow velocity by an external electric field. These high velocity particles impart momentum to the stagnant air particles in the separated region by frictional coupling. The momentum gained by the netural air particles will cause a reduction in the extent of the separated region. The efficient injection of the charged particles, which requires a small particle mobility, occurs in the most optimum way for particles of about one micron in radius (Ref. 6,7).

The amount of momentum possessed by a flow of charged particles in an electric field, and hence the maximum amount that can be transferred, can be related to the pressure generated by this flow. This electric pressure can be found (Ref. 13) for a one-dimensional system which, while not realistic, gives a feel for what is happening. Consider the flow of

a dielectric gas into which positive charges are injected and then accelerated as in Figure 1. The dielectric gas is considered incompressible and to be moving at a uniform velocity. At x=0 positive ions of constant mobility b are injected into the flow with a velocity equal to the flow velocity. The ions are accelerated toward the downstream collector under the influence of an electric field of intensity E. This field is generated by an external power supply which causes the potential at x=0 to be W_o, and at x=L to be W_L, where W_o is greater than W_L. The system is operated at a steady state in that all the ions injected at x=0 are collected at x=L and the external current I is constant. The remaining quantities are as given in the list of symbols. The governing equations for this system are

Conservation of Mass

$$\delta u A = \dot{M} \qquad 2\text{-}1$$

Conservation of Charge

$$\rho u A = I \qquad 2\text{-}2$$

Conservation of Momentum

$$\delta u \frac{du}{dx} + \frac{dp}{dx} - \rho E = 0 \qquad 2\text{-}3$$

Poisson's Equation

$$\frac{dE}{dx} = \frac{\rho}{\epsilon} \qquad 2\text{-}4$$

Potential Relation

$$-\frac{dW}{dx} = E \qquad 2\text{-}5$$

Current Density Equation

$$j = \rho(bE + u) \qquad 2\text{-}6$$

Substituting the space charge density as given by Eq. 2-4 into

Eq. 2-6 gives an equation relating the electric field intensity to the current density and the flow velocity,

$$j\,dx = \epsilon b\,(E + \frac{u}{b})\,dE \qquad 2\text{-}7$$

Since the external current is constant, the current density, which for unit depth is just the external current divided by the cross-sectional area of the channel, is a constant. Now, assuming that the flow velocity is independent of the field intensity Eq. 2-7 may be integrated. After evaluation of the constant of integration this equation can be solved for the field intensity to give

$$E = \left[2\,\frac{jx}{\epsilon b} + (E_o + \frac{u}{b})^2\right]^{\frac{1}{2}} - \frac{u}{b} \qquad 2\text{-}8$$

Since frictional effects are neglected, u=U, Eq. 2-10 may be differentiated with respect to x and substituted into Poisson's equation to yield an expression for charge density,

$$\varrho = \frac{j}{b}\left[\frac{2jx}{\epsilon b} + (E_o + \frac{u}{b})^2\right]^{\frac{1}{2}} \qquad 2\text{-}9$$

This equation along with Eq. 2-10 may be substituted into the momentum equation to give a differential expression for the pressure,

$$dp = \left[\frac{j}{b} - \frac{j}{b^2}\,U\left[\frac{2jx}{\epsilon b} + (E_o + \frac{U}{b})^2\right]^{\frac{1}{2}}\right]dx \qquad 2\text{-}10$$

After integrating, evaluating the constant, and simplifying, the pressure change caused by charge movement in the electric field may be written into final form

$$p - p_o = \frac{\epsilon}{2}\,(E^2 - E_o^2) \qquad 2\text{-}11$$

Taking $E_o = 0$ and $E = E_b = 3\times10^6$ volts per meter, the breakdown field for air at normal conditions, and using $\epsilon = 8.86\times10^{-12}$ ampere seconds per

volt meter the maximum pressure change that can be expected is approximately 40 newtons per square meter or 0.835 pounds per square foot.

Cheng (Ref. 5), as previously noted, suggests that a pressure increase of 1000 dynes per square centimeter, which is 100 newtons per square meter, will cause a turbulent boundary layer to remain attached for one additional meter. The maximum electric pressure as calculated above is a sizeable fraction of this value. This would seem to indicate that a significant boundary layer control might be achieved by this method.

If this maximum electric pressure is divided by a suitable dynamic pressure the resulting ratio may be compared to the parameter used by Stuetzer (Ref. 12) to indicate when flow modifications became noticeable in his experiments on flow control. The dynamic pressure chosen is that corresponding to a normal aircraft landing speed of 110 knots. For standard temperature and pressure this is 41 pounds per square foot. This ratio turns out to be about 0.02 while Stuetzer indicates that separation reduction became noticeable for a value of 0.03. Here it would appear that the possibility of causing a significant control is small. However, the comparison is made for two different mediums, air vice kerosene, so a strict comparison is not possible without additional information.

The ratio for air can be improved by increasing the maximum breakdown field strength, and this can be done in a number of ways. One way, which occurs naturally in a separated flow area, is to increase the turbulence level (Ref. 4). Another is the use of chemical additives such as sulphur hexafluoride (SF_6) or Arctron-12 (CCl_2F_2) (Ref. 3).

These compounds act as electron scavengers to decrease the number of free electrons in the field which in turn increases the breakdown field strength by as much as a factor of three. It is interesting to note that an increase in breakdown field strength of approximately seven kilovolts per centimeter (E_b = 37 x 10^6 volts per meter) would increase the ratio of electric pressure to dynamic pressure for air to 0.03, the value cited (Ref. 12) for noticeable separation reduction.

Another means of assessing the possibility of delaying separation by using ions or charged particles is to use the Navier-Stokes equations with an electric body force term included. Consider the two dimensional system as shown in Figure 2 in which positive charges are injected into an incompressible air flow, at the body surface, just upstream from the separation point. The ions are collected at some point downstream after being accelerated by an electric field. The field is generated by an external power supply which causes a potential difference between the injector and the collector. It is assumed that the currents involved are small and that the field effects take place in a small region near the body surface. The extent of this region is of the same order of magnitude as the size of the region in which viscous effects occur in the ordinary boundary layer assumptions. With this assumption, the flow may be separated into two regions, the outer where electric and viscous effects are negligible and the inner region where electric and viscous effects are of comparable size to the pressure and convective terms. The Navier-Stokes equations may then be written for each region

Outer Region

x Direction

$$U \frac{dU}{dx} = -\frac{1}{\delta} \frac{\partial p}{\partial x} \qquad 2\text{-}12$$

y Direction

$$\frac{\partial p}{\partial y} = 0 \qquad 2\text{-}13$$

Inner Region

x Direction

$$u \frac{\partial u}{\partial x} + v \frac{\partial u}{\partial y} = - \frac{1}{\delta} \frac{\partial p}{\partial x} + \frac{\varrho}{\delta} E_x + \frac{\nu}{\delta} \frac{\partial^2 u}{\partial y^2} \qquad 2\text{-}14$$

y Direction

$$\frac{1}{\delta} \frac{\partial p}{\partial y} = \frac{\varrho}{\delta} E_y \qquad 2\text{-}15$$

From Eq. 2-14 it is concluded that the pressure in the external flow region is independent of y so that the partial derivative of p with respect to x becomes a total derivative. The effects of the electric field in the y direction are small and may be neglected so that the change in pressure across the inner region is zero. As in the ordinary boundary layer approximations this implies that the external or potential flow pressure is impressed across the boundary layer. Right at the body surface both velocity components are zero so that Eq. 2-15 may be written

$$\left| \frac{1}{\delta} \frac{dp}{dx} - \frac{\varrho}{\delta} E_x \right|_{\text{wall}} = \left| \frac{\nu \partial^2 u}{\delta \partial y^2} \right|_{\text{wall}} \qquad 2\text{-}16$$

Separation occurs as the magnitude of the viscous term goes through zero. If this term could be made always to stay less than zero, separation could not occur. This can be accomplished if

$$\frac{\varrho}{\delta} E_x > \frac{1}{\delta} \frac{dp}{dx} . \qquad 2\text{-}17$$

Since the pressure gradient in the x direction can be related to the convective term of the potential flow, Eq. 2-17 may be written,

$$\frac{\varrho}{\delta} E_x > U \frac{du}{dx} . \qquad 2\text{-}18$$

As shown in Appendix A this condition at the surface is the maximum case. At points in the boundary layer away from the wall the convective terms cause a decrease in the value that the electric body force must assume to prevent separation. Thus, satisfying this criterion at the surface suffices for the whole boundary layer height.

To accelerate the boundary layer efficiently, the electric field strength and the charge density must be near the maximum possible. The maximum for each quantity would be that associated with conditions just before breakdown. For air at standard temperature and pressure the breakdown field strength, as given before, is 3×10^{6} volts per meter while the breakdown limited charge density is 4.5×10^{-3} coulombs per cubic meter (Ref. 7). Using these values the maximum that the electric body force per unit mass may attain is,

$$\left|\frac{\rho}{\delta} E_x\right|_{max.} = 1.1\times10^{4} \text{ m/sec}^2 .$$

In Appendix B values for the magnitude of the x component of the pressure gradient are calculated by equating to the potential flow convective term as in Eq. 2-12. This term is calculated for a circular cylinder, a Joukowsky airfoil, and for a NACA 0012 airfoil. These values are respectively 4.93×10^{3}, 1.33×10^{3} and 9.4×10^{2}, all with units meters per square second. In all three cases the maximum electric body force is approximately an order of magnitude larger than the convective term, or by Eq. 2-12 the pressure gradient.

From this it is seen that the electric body force term can be sufficiently large to cause the viscous term of Eq. 2-16 to stay negative. It is then concluded that it is possible to delay separation on a body in a decelerated flow region by electrogasdynamic interactions provided

the particles can be injected in sufficient quantity and proper size to insure optimum conversion and maximum density, and that early breakdown and current leakage are prevented.

III. EXPERIMENTAL APPARATUS AND EXPERIMENTAL PROCEDURE

A. EXPERIMENTAL APPARATUS

This research was begun with the intention of demonstrating that a region of separated flow on an airfoil could be affected by the injection and acceleration of charged particles, but because of design and test difficulties it was necessary to begin with a test apparatus that was more compatible with the small size of the existing EGD tunnel facility, Since the tunnel is two inches by four inches in the inlet cross section, the airfoil would necessarily have been very thin to preclude tunnel blockage. This would have made it virtually impossible to route supply and instrumentation leads through the model cross section. The thinness of the airfoil would also have eliminated any region of gross separation and the separation point would have been difficult to fix. The apparatus, selected to minimize these problems, finally settled upon was a backward facing step mounted in one wall of the test section as shown in Figure 3. This set up eliminated the above problems since any lines going into it needed only to be routed through the wall, the location of the step fixed the point of separation, and the extent of the separated region was comparable to the step height. While this apparatus solved some of the design difficulties it somewhat changed the method of attacking the question at hand. With an airfoil it was possible to ask if electro-gasdynamic interaction would delay separation, but with the step it was only possible to ask if reattachment could be hastened by these interactions. It was felt that the mechanism of momentum addition needed to cause a reduction in reattachment length was similar to that necessary to cause a separation delay, and that a demonstration of this reduction

could show the feasibility of electrogasdynamic interaction for separation control.

The backward facing step was made as an integral part of a detachable test section wall. Provision was made to mount three electrogasdynamic injector nozzles (Figure 4), of a type designed to produce micron-size charged water droplets (Ref. 8), on the step face to discharge particles downstream. Since these nozzles required a supply of saturated steam, at 250°F, to operate it was necessary to use a material for the step wall that would not only be a good electric and heat insulator but also maintain its strength at this temperature. Teflon filled both of these requirements and was used for the step wall, while plexiglass was used for the remaining three sides of the test section. Two compartments were milled out on the step wall, in the area upstream from the step (Figure 5A), to serve as a common plenum for the three nozzles, and to provide mounting room for the three corona needles. The plenum was sealed with a fiber reinforced phenolic cover into which three fittings, for supply and instrumentation lines, were mounted (Figure 5B). The inside dimensions of the finished test section were 2 by 4 inches in the 3 inch long inlet section, and 2.281 by 4 inches in the 6.25 inch long section downstream of the step. Two interchangeable inner surfaces, as shown in Figures (6A-6B), were made for the downstream section. Both of these were made of 0.094 inch thick teflon sheet, but one was smooth and drilled for pressure taps while the other was tufted with number 30 silk thread in an interlocking one-eighth inch grid pattern covering a three by three inch area immediately downstream of the step. The test section was mounted through a reducer to an air plenum in which screens and honeycombs were installed to reduce the flow turbulence and to insure

flow uniformity (Figure 7).

Tunnel air was supplied by a Carrier three stage centrifugal compressor capable of continuously supplying 4000 cubic feet of air per minute. The EGD nozzles could be supplied either with air from the laboratory's high pressure air supply, or with saturated steam from a commercial steam generator. This generator was extensively reworked to provide clean steam at a higher continuous flow rate. This rework included fabrication of a new boiler and a constant water-level supply valve of stainless steel to replace the mild steel components of the original design. All steel fittings and connections in the supply water and steam lines were replaced with non-ferrous parts. The steam line from the generator to the steam plenum was then wrapped with an electric heating tape and covered with insulation. The output capacity of the unit was increased by installing an additional calrod heating element in the boiler. With these modifications the generator was capable of providing a continuous supply of clean steam while maintaining a plenum pressure of 15 psig. A schematic of air and steam flow is shown in Figure 8.

The corona rings of the three nozzles, mounted at the nozzle exit plane, were connected in series to a Sorensen high voltage power supply capable of supplying 30 kilovolts. The needle of each unit was connected to a common ground. A collector wire (0.015 inch diameter steel piano wire) was mounted across the tunnel 0.3 of an inch downstream from the nozzle exit plane and 0.187 inch from the wall. This collector wire could be maintained at a high positive potential by a Spellman high voltage power supply also capable of producing 30 kilovolts. Both electric power supplies had built-in voltmeters with 0-30 kilovolt scales

and milliammeters with 0-50 milliamp scales but to provide more sensitive current readings, it was necessary to connect externally a Simpson microammeter with a 0-50 microamp scale. On the Sorensen unit, which supplied the corona potential, a Singer electrostatic voltment, which measured 0-40 kilovolts in four steps of 10 kilovolts each calibrated to 1% of full scale, was connected externally to provide finer measurement of the corona voltage. A Simpson microammeter was connected in series between each corona needle and ground. Figure 9 shows a schematic of the electric circuitry.

Thermocouples were installed in the steam plenum and on the electric heating tape to furnish temperature data from these two places. Conventional 0-50 psig pressure gages were used to read out pressure in the nozzle plenum and in the steam and air supply lines. A water manometer, connected to a traversable pitot static tube, was used to measure the flow pressure of tunnel air. A series of 19 pressure taps, at a half inch on either side of the center nozzle, spaced at intervals of one-eighth of an inch, were installed in the wall starting three-eights of an inch downstream from the step. These taps, used to record the static pressure at the wall in the separated regions, were connected to a water manometer bank. A Securities Associates two-channel hot wire anemometer and a traverse unit were available to obtain velocity information. It was necessary to modify the traverse unit by extending the probe arm and to design and construct a positioning track. Details of the experimental setup are shown in Figures 10-12.

B. EXPERIMENTAL PROCEDURE

The procedures developed for this experiment were designed to evaluate how the reattachment point, for the separated flow over the backward facing step, moved as a result of adding momentum to the flow

through the nozzles. Then, by applying this information to the movement caused by an electrogasdynamic interaction, the amount of momentum being supplied by this method could be measured.

Three devices were used to obtain reattachment point information. These were hot-wire surveys, tuft observations, and static wall pressure profiles. It was realized that the hot wire could not be operated in a flow containing water droplets and/or charged particles; therefore, only air was injected through the nozzles during these runs. The tuft observations were intended to give mainly qualitative information but it was hoped that some approximate quantitative information might also be gained from these observations. It was anticipated that the static pressure profiles along the wall in the separated region would give the most accurate information for all types of nozzle flow.

Table 1 gives a summary of the various runs made with the information pertinent to each run. All runs were made with a tunnel air flow dynamic pressure of 20 centimeters of water which corresponds to a free stream velocity of 183 feet per second. I_c is the average corona current, I_L is the collector current and V_c is the accelerator voltage applied to the collector wire.

Run 1 was made to become familiar with the apparatus and to obtain some general information on the extent of the separated region. Run 2 was made to verify the flow uniformity in the inlet section. Run 3 was a series of velocity traverses at $z = \pm 0.5$ (see coordinate system of Figure 13) starting at the step and proceeding downstream past the reattachment point as shown by Run 1. Run 4 was a repeat of Run 3 with air flow through the nozzles and a nozzle plenum pressure of 7.5 psig. Run 5 was done to obtain a series of pressure profiles for various nozzle

plenum pressures to show reattachment point movement. Tuft pattern photos with steam injection through the nozzles were done in Run 6 to accomplish the same purpose. In Run 7 steam at the pressures listed was injected through the nozzles and then the pressures at the wall were recorded. The coronas of the three nozzles were then energized so that each was conducting, accelerator voltage was applied and the readings of the wall pressure taps were again taken.

RUN	NOZZLE FLOW	NOZZLE Plenum Pressure (psig)	I_c	I_L	V_L	Data Taken
1	None	0	0	0	0	Visual Tuft Observations
2	None	0	0	0	0	Hot wire velocity profiles
3	None	0	0	0	0	Hot wire velocity profiles
4	Air	7.5	0	0	0	Hot wire velocity profiles
5	None	0	0	0	0	Pressure profiles
	Air	2.5	0	0	0	" "
	Air	5.0	0	0	0	" "
	Air	7.5	0	0	0	" "
	Air	10.0	0	0	0	" "
	Air	12.5	0	0	0	" "
	Air	15.0	0	0	0	" "
6	None	0	0	0	0	Tuft Photography
	Steam	2.5	0	0	0	" "
	Steam	5.0	0	0	0	" "
	Steam	7.5	0	0	0	" "
7	None	0	0	0	0	Pressure Profiles
	Steam	2.5	0	0	0	" "
	Chgd. part.	2.5	28	50	8	" "
	Steam	5.0	0	0	0	" "
	Chgd. part.	5.0	28	50	8	" "
	Steam	7.5	0	0	0	" "
	Chgd. part.	7.5	28	50	8	" "

TABLE 1

SUMMARY OF EXPERIMENTAL PROCEDURE

V. RESULTS AND CONCLUSIONS

A. RESULTS

The observation of the tuft pattern made during the first run showed a fairly well defined reattachment line across the wall at about 1.375 inches downstream from the step. Since the line was straight, it appeared that the presence of the nozzles on the step was washed out due to turbulent mixing. This value for the reattachment distance was later used as a guide in locating the reattachment point with the velocity surveys.

Velocity traverses made in the inlet section show the flow to be uniform and to have a flat profile (Figure 14) similar to the profile that would be expected on a flat plate. This occurs for flow in an inlet of a rectangular duct that is not fully developed. Fully developed turbulent flow in an inlet section cannot be expected for at least 25 hydraulic diameters from the inlet, and in this case the complete inlet section was only about one hydraulic diameter long. The flow is assumed to be turbulent in the inlet since previous tests of a similar test section show the turbulent intensity of the flow at the inlet to be 0.14% and the boundary layer to be growing according to the 1/7th power law. At the step the profiles have developed a slight bulge near the wall (Figure 15A-B) so that a maximum velocity of 1.01 times the center-line velocity occurs at 0.25 inches from the wall. This is attributed to the influence of the lower pressure in the separated region below the step.

A minimum velocity existed, in each velocity survey made in the separated region, at some distance away from the wall. The (x,y) coordinates of this minimum velocity of each profile are shown in Figure 16.

A separated area behind a backward facing step is characterized by a two-dimensional recirculation velocity (Ref. 1) that runs upstream parallel to and near the wall and downstream next to the expanding channel flow. The existence of this minimum is interpreted as indicating that the velocity decreases to zero near the center of the separated region and then goes to some negative value near the wall. The point where the minimum velocity occurred at the wall (there was no inflection in the profile) was taken as the point of reattachment. This occurred for the condition of no nozzle flow at x = 1.37 inches and for a nozzle flow of air, at 7.5 psig plenum pressure, at x = 1.01 inches. The reattachment occurs for both cases at the same downstream point for z = $\pm$0.5 as shown in Figures 17-20.

As described in Ref. 1, a stall region downstream of a backward facing step has an over-all length of separation based on the point where the edge of the expanding flow first contacts the wall. This point is a short distance downstream from the end of the two-dimensional recirculation region. This is shown in Figure 21 which is taken directly from Ref. 1. The nomenclature "first point of reattachment" and "re-attachment point" is new and will be used hereafter in describing these points. The data obtained from the velocity surveys are correlated with the first point of reattachment since it occurs immediately after the region of recirculation flow.

The data obtained from the static pressure taps show a negative velocity just below the step which gradually increases to a maximum positive pressure and then drops off. To analyze what is happening here, it is helpful to look at Figure 21. In the three-dimensional flow region and the recirculation region there is a flow velocity near the wall.

Hence in these regions the static pressures will be negative. Just before the first point of reattachment the pressure will go to zero since there will be a point of zero flow velocity. Between the first point of reattachment and the reattachment point more of the channel flow will impinge on the wall causing an increase in pressure. At the reattachment point this pressure will be a maximum and will gradually decrease as the flow realigns to become nearly parallel again.

The pressure profiles for the separated flow and for the separated flow with air injection through the nozzles at various pressures are shown in Figure 22. The x-coordinate of the first point of reattachment and that of the reattachment point are cross plotted from Figure 22 onto Figure 23 which has as ordinate the thrust produced by the three nozzles per unit nozzle exit area. The method of calculating the thrust produced by these nozzles is shown in Appendix C.

Since the movement of the reattachment points was more pronounced at the lower values of thrust addition it was decided to operate at these lower values for steam and charged particle injection.

The next run was made using the tufted inner wall and injecting steam to find out how valuable this measurement technique was. As can be seen from Figures 24-25, the information was mostly qualitative. The reattachment line was much clearer in an airflow since the steam wet the threads so that they were not as sensitive when steam was injected.

The pressure profiles obtained with the steam injection are shown plotted as smooth curves in Figure 26. Immediately after the data were obtained with the steam injection at each plenum pressure setting, the corona units were energized to two kilovolts and adjusted for operating at steady currents. The corona currents were different on each nozzle,

being approximately 50, 25, and 10 microamps respectively on nozzles 1, 2, and 3. However, the spacing of the needles was so critical in regard to corona current that this range was the best that could be obtained with the apparatus. The accelerator potential on the collector was raised to 8 kilovolts, the highest that could be maintained without breakdown. The collector current for this condition was about 50 microamps. Then the static pressures along the wall were read again. These values are plotted as points on Figure 27. As can be seen most of these points fall right on the associated curve so that no change is evident. In order to determine if a change in these static pressure values was taking place that was smaller than the least count of the manometer board (0.1 centimeters of water or 0.205 pounds per square foot), a micromanometer that measured to the nearest 0.01 centimeters of water was connected to various taps. The fluctuation of the setup was approximately 0.08 centimeters of water and at no time did the injection and acceleration of the charged particles cause a pressure change greater than 0.05 centimeters of water. The manometer change associated with the maximum electric pressure of 0.835 pounds per square foot is 0.4 centimeters of water.

B. CONCLUSIONS

The experimental values of charge density and breakdown field intensity with steam injection as calculated in Appendix D are 6.4×10^{-4} coulombs per cubic meter and 8.5×10^{5} volts per meter respectively. These values were found using the assumption of a homogeneous one-dimensional field. The breakdown field strength is lower than that cited previously because the experimental field was not actually one-dimensional and homogeneous, and because a space charge was present. The breakdown

field for this apparatus in quiet air is 11.6×10^5 volts per meter so that the increase in breakdown field strength due to turbulence is not evident, possibly due to the presence of moisture.

The charge density calculated from Poisson's equation, which is done without assuming a particle size or mobility, is very close to the charge density calculated from the current density equation, which was done assuming a 1 micron particle radius. This implies that the EGD injector nozzles are producing particles which can be efficiently coupled to a viscous flow. In fact, the greatest proportion of the collector current obtained was due to the convective movement of the particles as seen by noting that the mean flow velocity was 384 meters per second while the drift velocity was only 4 meters per second.

The electric pressure that was calculated from the experimental field intensity corresponds to a manometer change of 0.03 centimeters of water. Thus, the pressure that was generated by the charged particle drift velocity was completely lost in the pressure fluctuations due to the turbulent component of the flow velocity. This can also be seen by noting the great difference in mean flow velocity and drift velocity.

Therefore, it is concluded that no movement of the reattachment point was observed because the magnitude of the momentum addition due to electrogasdynamic interaction was too small to cause a detectable change.

The backward facing step provides a well-defined separated region. The reattachment point for this kind of separated flow is quite sensitive to momentum addition. The movement of the reattachment point was four inches per pound of injected thrust for low thrust levels, but decreased rapidly as the injected thrust increased. This damping out of the reattachment point movement was due to the fact that the discharge area

was only a small fraction of the step area and that at higher thrust levels the injected flow became more turbulent and less efficient in imparting momentum in a downstream direction.

VI. RECOMMENDATIONS

The experiment should be redesigned to allow operation in the region where small values of injected momentum cause large changes in the reattachment length. This could be done in a setup using a flow of air, saturated with water vapor, over a backward-facing step. A corona discharge device could be mounted in the separated area immediately downstream of the step. This device should not require steam injection to operate it, thus eliminating the movement of the reattachment point by any means other than EGD interactions. Part of the device might even be on the face, for instance a wire on the face and a half cylindrical screen slightly downstream. The saturated air entering this separated area would condense in the region of the discharge and obtain a charge. A field applied between the corona and some downstream collector would cause these particles to be accelerated toward the collector. Care should be taken to keep the field as one-dimensional as possible to ensure a breakdown intensity near maximum. This would also allow the attainment of higher charge densities. The area that the corona discharges into should be of the same size as the step face.

It would be worthwhile to make an investigation of reattachment point movement by injection beneath various height steps. This investigation might indicate a particular size step that was more sensitive to momentum injection. In this investigation a more thorough survey of the separated area could be made to find the extent of the three-dimensional region (Figure 22) immediately downstream of the step (Ref. 1), to determine if a particular location or configuration of corona device could take advantage of this flow.

The pressure taps along the wall were the only reliable means of obtaining reattachment point information with steam injection but they had a tendency to become plugged because of condensation inside the taps. A multiple trap arrangement should be constructed so that each pressure tap is connected to the manometer through a trap. These traps would collect the condensate without allowing the taps themselves to become plugged. Another solution to this problem would be to make the taps out of teflon tubing. Since teflon is a poor conductor, the steam would not condense in them as it does in metal tubes. Then mount the test channel with the step at the top. Since water does not "wet" teflon, the condensate that forms in the teflon tubes would then fall out. A third solution would be to use a series of pressure transducers mounted in the wall.

APPENDIX A

EFFECT OF CONVECTIVE TERMS

It has been shown that the value of the electric body force term to prevent separation at the body surface is

$$\left|\frac{\varrho E_x}{\delta}\right| > \left|\frac{1}{\delta}\frac{dp}{dx}\right| \qquad \text{A-1}$$

At a position in the boundary layer away from the wall and at the same stream-wise distance, the x-momentum equation is

$$\frac{1}{\delta}\frac{dp}{dx} - \frac{\varrho}{\delta}E_x + u\frac{\partial u}{\partial x} + v\frac{\partial u}{\partial y} = \nu\frac{\partial^2 u}{\partial y^2} \qquad \text{A-2}$$

This equation can be rewritten using the continuity equation

$$\frac{\partial u}{\partial x} + \frac{\partial v}{\partial y} = 0 \qquad \text{A-3}$$

Then equation B-2 becomes,

$$\frac{1}{\delta}\frac{dp}{dx} - \frac{\varrho}{\delta}E_x - u\frac{\partial v}{\partial y} + v\frac{\partial u}{\partial y} = \nu\frac{\partial^2 u}{\partial y^2} \qquad \text{A-4}$$

which can be written,

$$\frac{1}{\delta}\frac{dp}{dx} - \frac{\varrho}{\delta}E_x - u^2\frac{\partial}{\partial y}\left(\frac{v}{u}\right) = \nu\frac{\partial^2 u}{\partial y^2} \qquad \text{A-5}$$

As before, no separation can occur if the term on the right hand side stays negative. The quantity in parenthesis is negative by equation A-1 and is made more negative by the last term since v/u is the stream-line slope which increases from zero at the body surface to a maximum at the boundary layer edge as seen from the flat plate solution (Ref. 9). Then the criterion for prevention of separation at points away from the body is

$$\left|\frac{\varrho E}{\delta}x\right| > \left|\frac{1}{\delta}\frac{dp}{dx} - v^2\frac{\partial}{\partial y}\left(\frac{v}{u}\right)\right| \qquad \text{A-6}$$

which is less stringent than the requirement at the wall.

APPENDIX B

CALCULATION OF THE PRESSURE
GRADIENT TERM OF THE NAVIER-STOKES EQUATION

1. Circular Cylinder

For the potential flow about a right circular cylinder the flow velocity is given by (Ref. 14)

$$U^2 = U_\infty^2 \left[1 - \frac{a^4}{r^4} + 2\frac{a^2}{r^2}\left(\sin^2\theta - \cos^2\theta\right)\right] \qquad \text{B-1}$$

where a is the cylinder radius and $\sin\theta = \frac{y}{r}$ and $\cos\theta = -\frac{x}{r}$.

Then for the velocity at the surface, where r=a,

$$U^2 = 2\,U_\infty^2 \left[1 + \left|\frac{y^2 - x^2}{x^2 + y^2}\right|\right] \qquad \text{B-2}$$

Differentiating this quantity with respect to x,

$$2\,U\frac{du}{dx} = 2\,U_\infty^2 \left[\frac{(x^2 + y^2)(-2x) - (y^2 - x^2)\,2x}{(x^2 + y^2)^2}\right] \qquad \text{B-3}$$

Simplifying this expression and relating it to the pressure gradient,

$$\frac{1}{\rho}\frac{dp}{dx} = -U\frac{du}{dx} = 4\frac{U_\infty^2\, x\, y^2}{r^4} \qquad \text{B-4}$$

Choosing a cylinder of unit radius and a free stream velocity of 110 kts or 56 meters per second B-4 may be rewritten in terms of .

$$\frac{1}{\rho}\frac{dp}{dx} = -1.25 \times 10^4 \cos\theta \sin^2\theta \qquad \text{B-5}$$

The maximum value of this equation is found in the usual way to occur at $\theta = 125.7^\circ$ where $\cos\theta = -0.58$, $\sin\theta = 0.82$. Then the maximum magnitude of the pressure gradient is

$$\left(\frac{1}{\rho}\frac{dp}{dx}\right)_{max} = 4.93 \times 10^3 \ \text{m/sec}^2 \qquad \text{B-6}$$

2. Joukowsky Airfoil

The value of the pressure gradient for this case is calculated by using graphical data as found in Ref. 7. Separation occurs at x = 0.47C and at this point the slope of the graph of dimensionless velocity versus dimensionless chord-wise distance is

$$\frac{d\left|\frac{U}{U_\infty}\right|}{d\left|\frac{x}{c}\right|} = -0.36$$ and the value of

the velocity at this point is $U = 1.1U_\infty$. Then approximately

$$U\frac{dU}{dx} = -0.435\frac{U_\infty^2}{c} \qquad \text{B-7}$$

but, as before,

$$\frac{1}{\delta}\frac{dp}{dx} = -U\frac{du}{dx} = 0.435\frac{U_\infty^2}{c} \qquad \text{B-8}$$

Using U_∞ = 56 meters per second and c = 1 meter, the pressure gradient near the separation point is approximately

$$\frac{1}{\delta}\frac{dp}{dx} = 1.33 \times 10^3 \text{ m/sec}^2$$

3. NACA 0012 Airfoil

In Ref. 2 on page 321, $\left(\frac{U}{U}\right)^2$ versus $\left(\frac{x}{c}\right)$ is plotted for an NACA 0012 airfoil. The slope of this curve is approximately constant from $\frac{x}{c}$ = 0.2 to $\frac{x}{c}$ = 0.8 at

$$\frac{d\left|\frac{U}{U_\infty}\right|^2}{d\left|\frac{x}{c}\right|} = -0.6$$

Performing the indicated differentiation and simplifying,

$$U\frac{dU}{dx} = -0.3\frac{U_\infty^2}{c} \qquad \text{B-9}$$

Then using U=56 meters per second and c=1 meter

$$\frac{1}{\delta}\frac{dp}{dx} = 9.4 \times 10^2 \text{ m/sec}^2.$$

APPENDIX C

CALCULATION OF NOZZLE THRUST

The thrust produced by a flow through a convergent nozzle is given by (Ref. 11),

$$\frac{T}{A^*} = 2\left[\left(\frac{2}{k+1}\right)^{\left(\frac{1}{k-1}\right)}\right] p_o - p_a \qquad \text{C-1}$$

Denoting the nozzle plenum pressure by p_g to indicate that it is a gage pressure, this expression may be written in terms of the gage pressure in the plenum as

$$\frac{T}{A^*} = 2\left[\left(\frac{2}{k+1}\right)^{\left(\frac{1}{k-1}\right)}\right] p_g + 2\left[\left(\frac{2}{k+1}\right)^{\left(\frac{1}{k-1}\right)} - 1\right] p_a \qquad \text{C-2}$$

For steam with $k=1.33$ and $p_a=14.7$ psi, this becomes

$$\left(\frac{T}{A^*}\right)_s = 1.264p_g + -.264p_a \qquad \text{C-3}$$

For air with $k=1.4$ and $p_a = 14.7$ psi, it is

$$\left(\frac{T}{A^*}\right)_A = 1.246p_g + 0.246p_a \qquad \text{C-4}$$

Table II shows the thrust per unit discharge area developed at each plenum pressure used.

TABLE II

THRUST DEVELOPED BY CONVERGENT NOZZLE FOR AIR AND STEAM AT VARIOUS PLENUM PRESSURES

Plenum Pressure (psig)	T/A* Air (psi)	T/A* Steam (psi)
2.5	6.72	7.04
5.0	9.83	10.20
7.5	12.94	13.36
10.0	16.05	16.52
12.5	19.16	19.68
15.0	22.27	22.84

APPENDIX D

CALCULATION OF ELECTRIC BODY FORCE AND PRESSURE FROM EXPERIMENTAL VALUES

Breakdown occurred between the collector and the corona ring at a collector potential of 8.5 kilovolts and a corona potential of 2.0 kilovolts. The distance separating the ring and the collector is 7.62×10^{-3} meters. The linear homogeneous breakdown intensity is then,

$$\left|E_b\right| = \frac{dW}{dx} = 8.5 \times 10^5 \ \frac{\text{volts}}{\text{meter}} \qquad \text{D-1}$$

The the electric pressure due to this field is,

$$p = \frac{\epsilon}{2} E_b^2 = 3.2 \ \frac{\text{newt}}{\text{meter}^2} = 0.067 \ \frac{\text{pounds}}{\text{feet}^2} \qquad \text{D-2}$$

From Poisson's equation the charge density is,

$$\rho = \epsilon \frac{dE}{dx} = 9.9 \times 10^{-4} \ \frac{\text{coulombs}}{\text{meter}^3} \qquad \text{D-3}$$

The charge density can also be calculated using the current density equation,

$$\frac{I_c}{A} = \rho (bE+u) \qquad \text{D-4}$$

Assuming that the EGD injector nozzles are operating at design conditions, so that they are injecting singly charged particles of 1 micron radius, the particle mobility will be 5×10^{-6} square meters per volt second (Ref. 4). From this the drift velocity is 4.25 meters per second. The flow velocity at nozzle exit is sonic and may be calculated (Ref. 11) to be 384 meters per second. As seen from Figures 24-25 the discharge jet width increases only slightly from exit to collector wire. With the drift velocity very much smaller than the flow velocity the one-dimensional continuity equation holds approximately. Thus, using an exit velocity of 384 meters per second, an exit area of 4.64×10^{-4}

square meters the charge density is,

$$\rho = 2.8 \times 10^{-4} \frac{\text{coulombs}}{\text{meter}^3} \qquad \text{D-5}$$

This compares favorable to the value found from Poisson's equation,

Using an average of these two charge densities to compute the electric body force,

$$\frac{\rho}{\delta} E_b = 4.4 \times 10^2 \frac{\text{meters}}{\text{seconds}^2} \qquad \text{D-6}$$

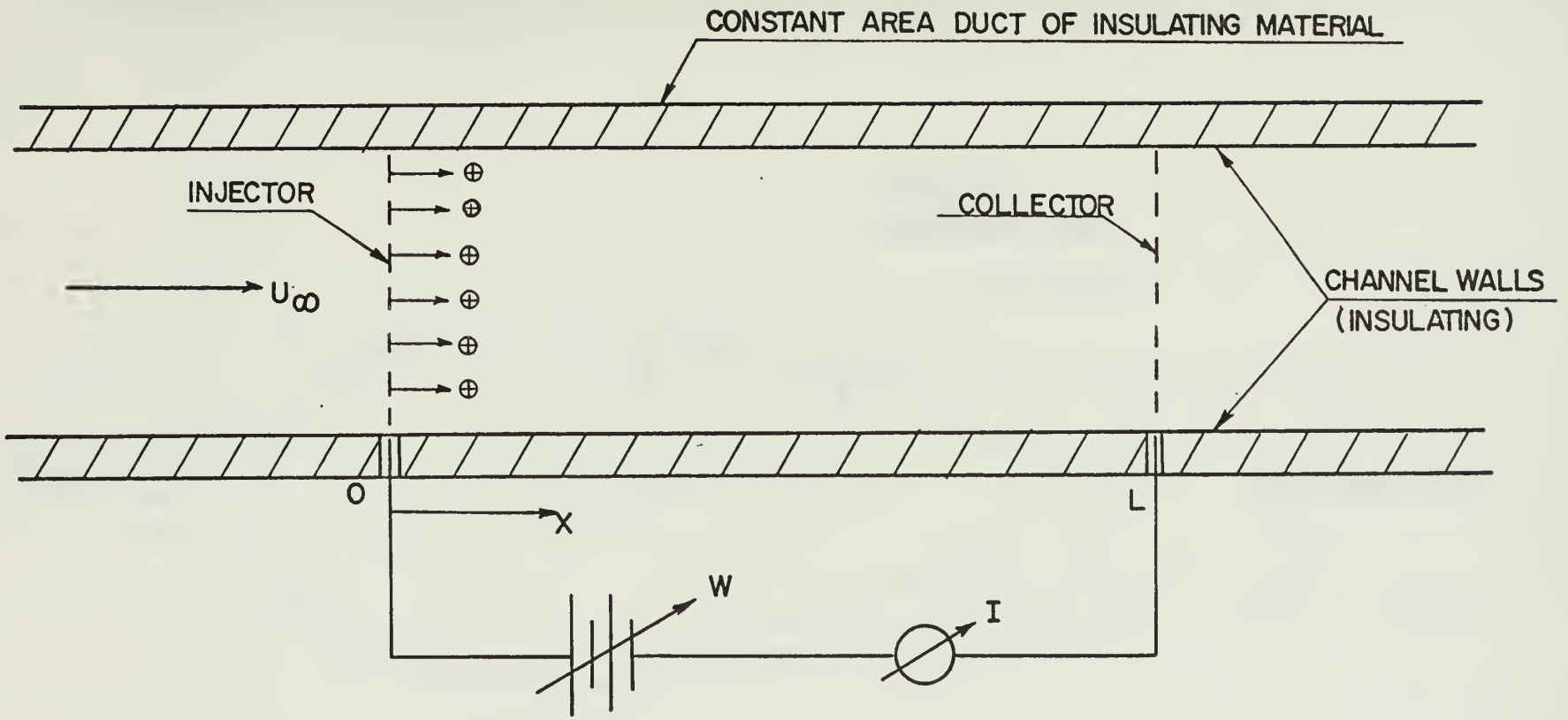

FIGURE 1

SYSTEM FOR DEVELOPING ELECTRIC PRESSURE.

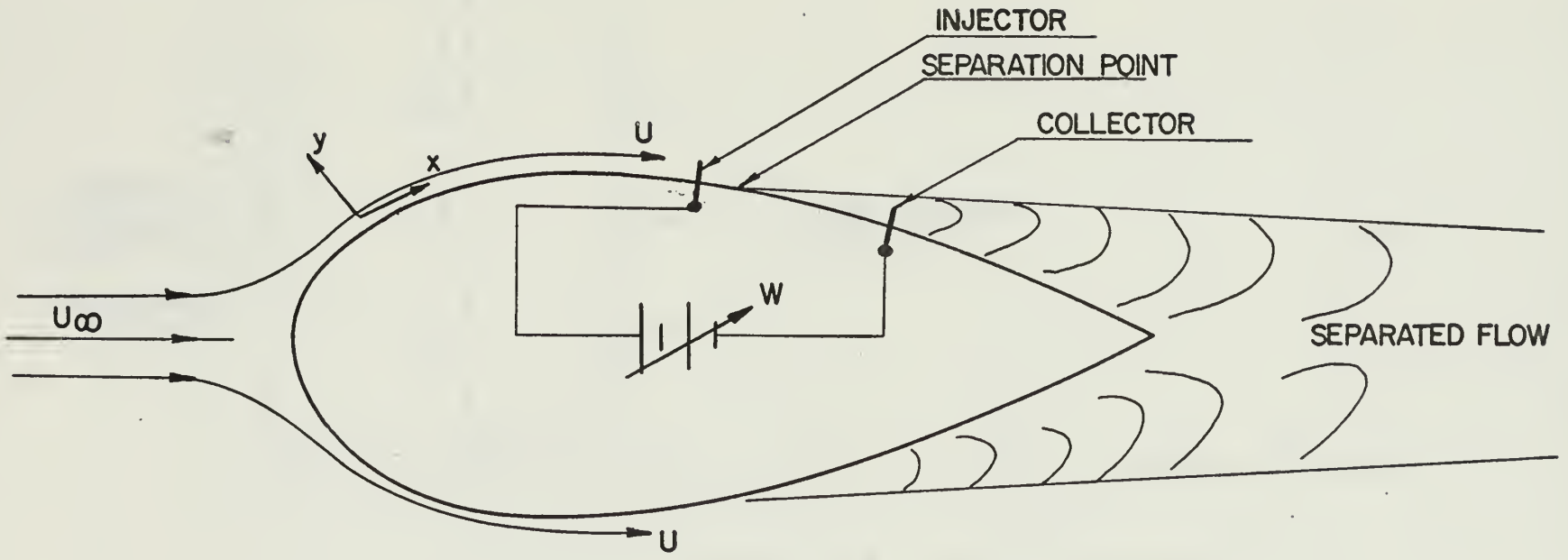

FIGURE 2

SYSTEM FOR DERIVING BOUNDARY LAYER EQUATIONS
WITH ELECTRIC BODY FORCE.

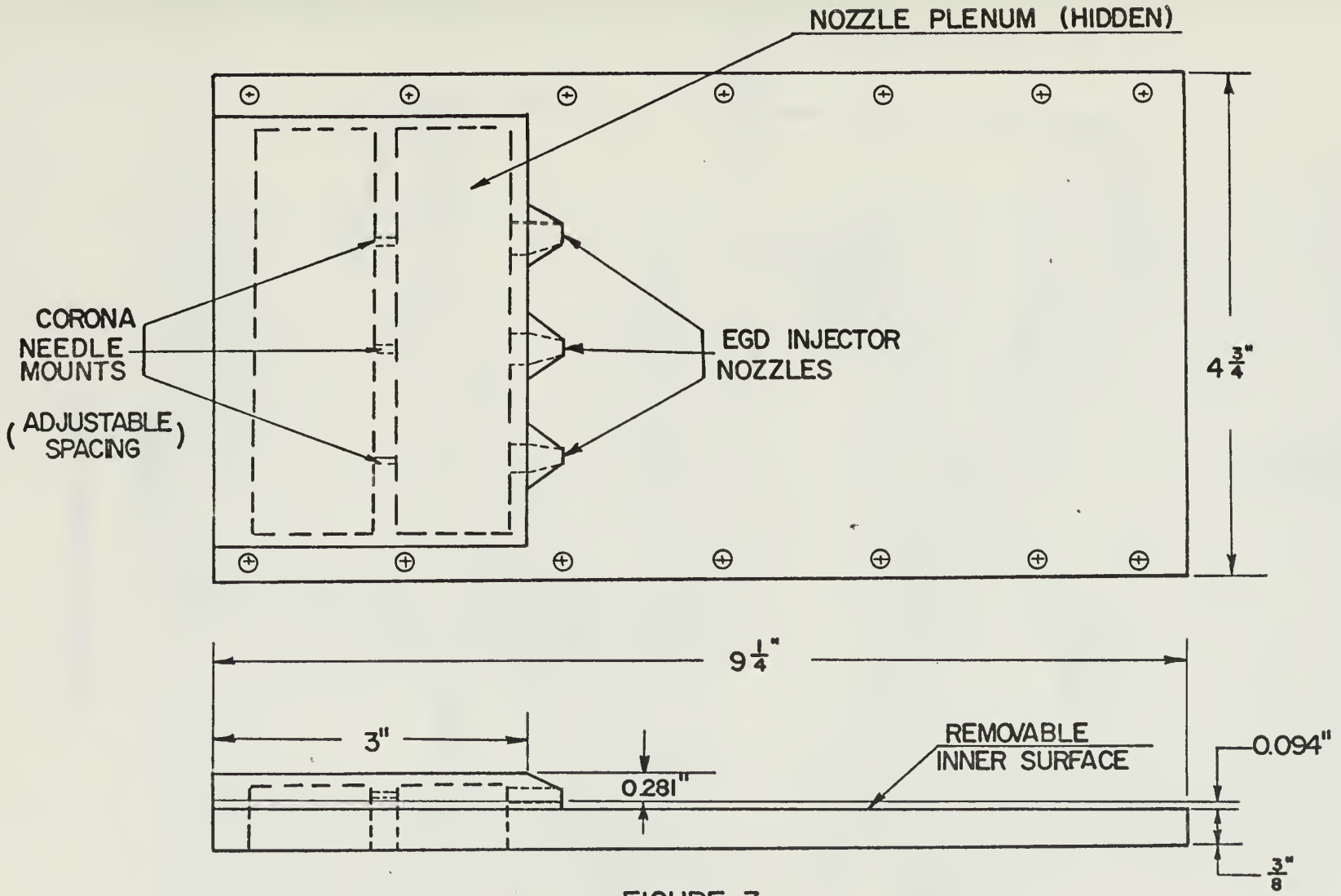

FIGURE 3

STEP WALL INSERT.

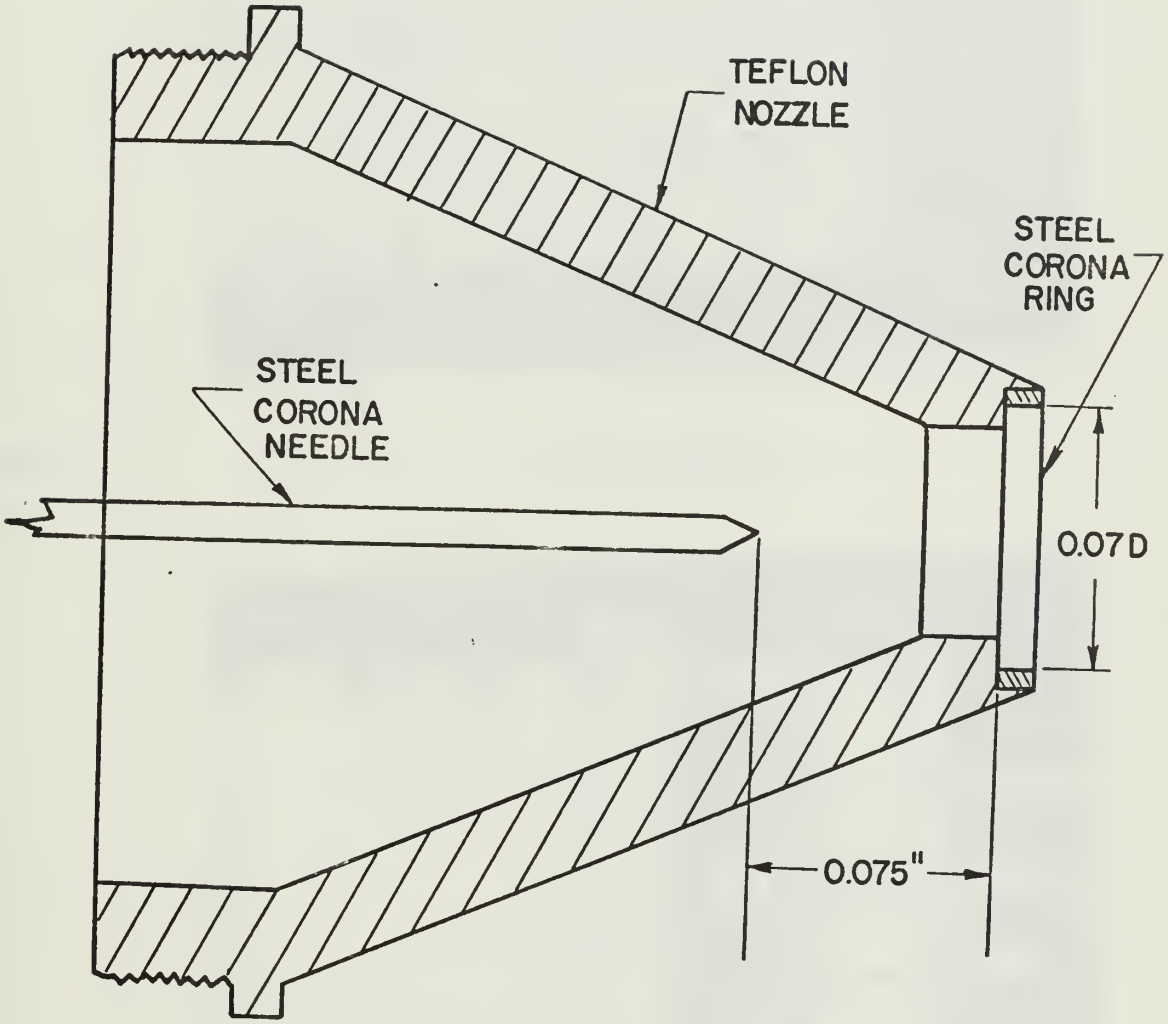

FIGURE 4

EGD INJECTOR NOZZLE

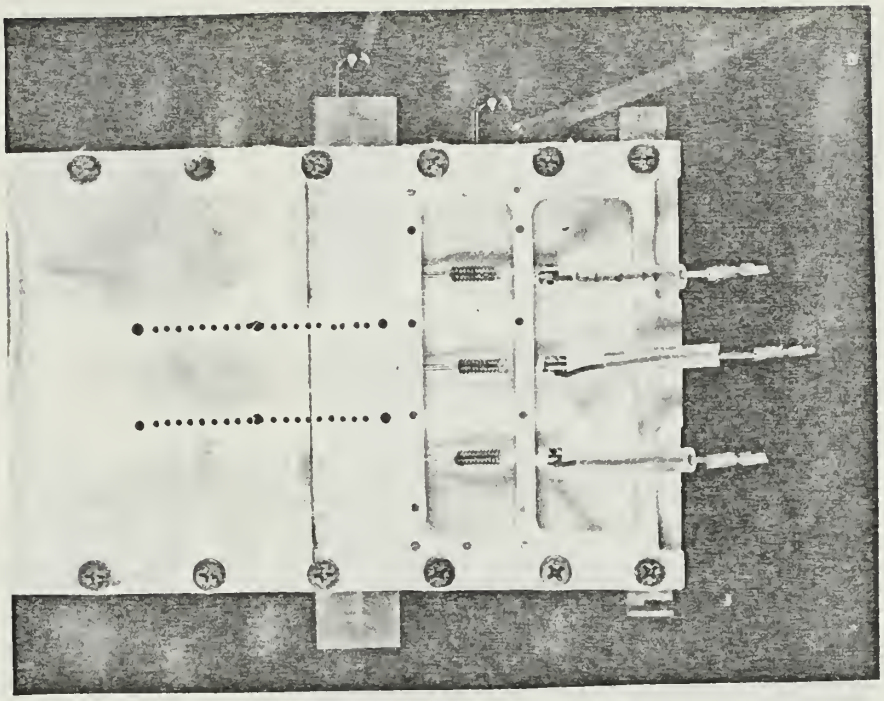

FIGURE 5A NOZZLE PLENUM

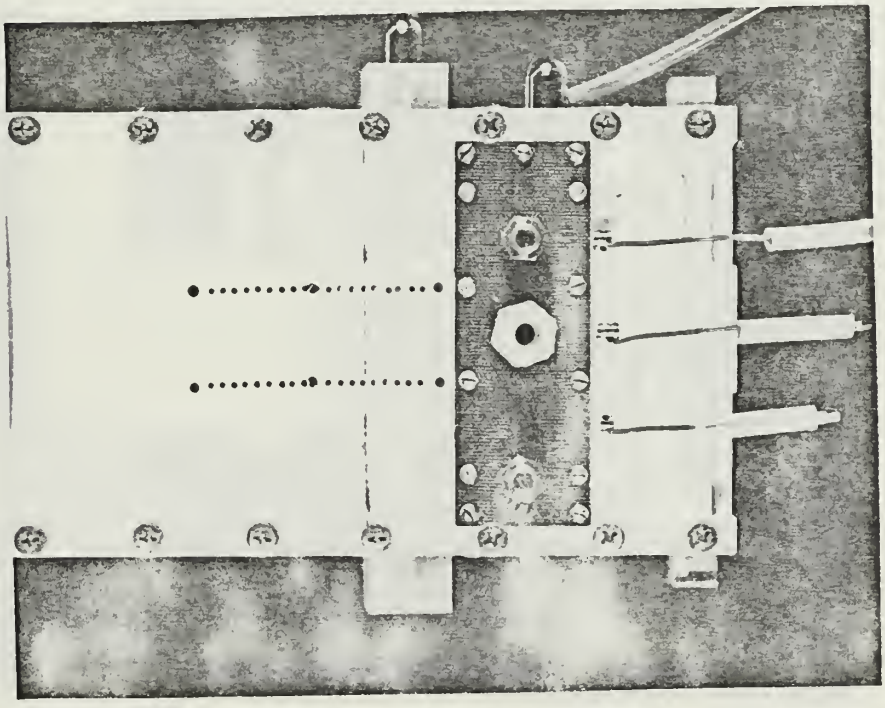

FIGURE 5B NOZZLE PLENUM COVER

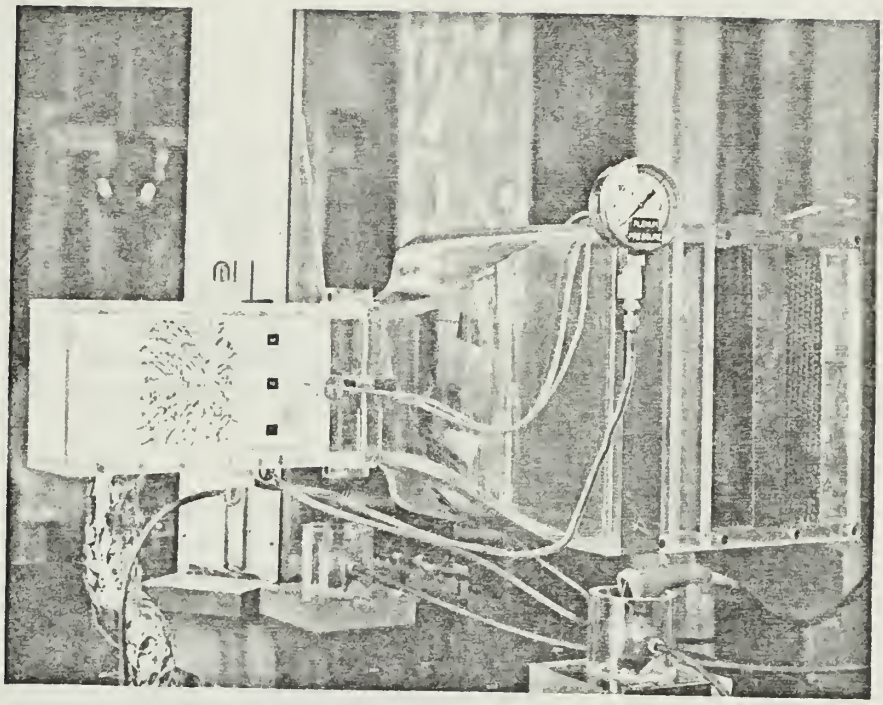

FIGURE 6A SECTION WITH TUFTED WALL

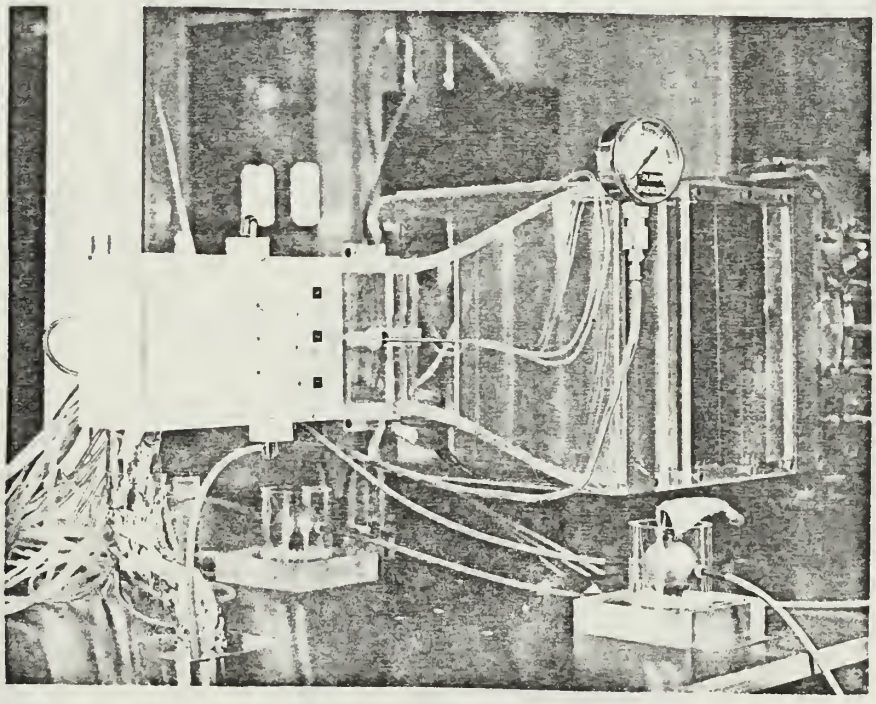

FIGURE 6 B SECTION WITH SMOOTH WALL

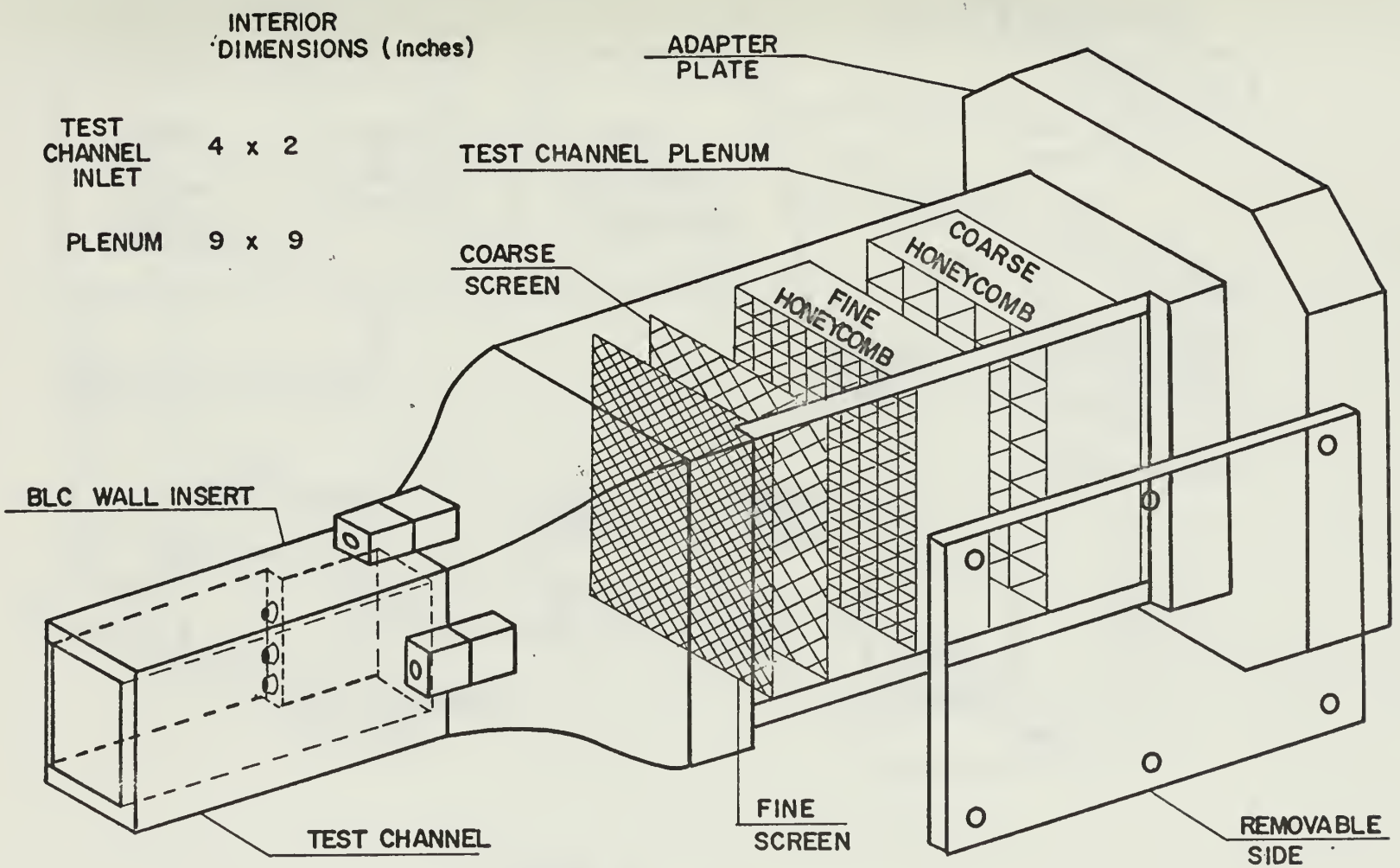

FIGURE 7
TEST SECTION

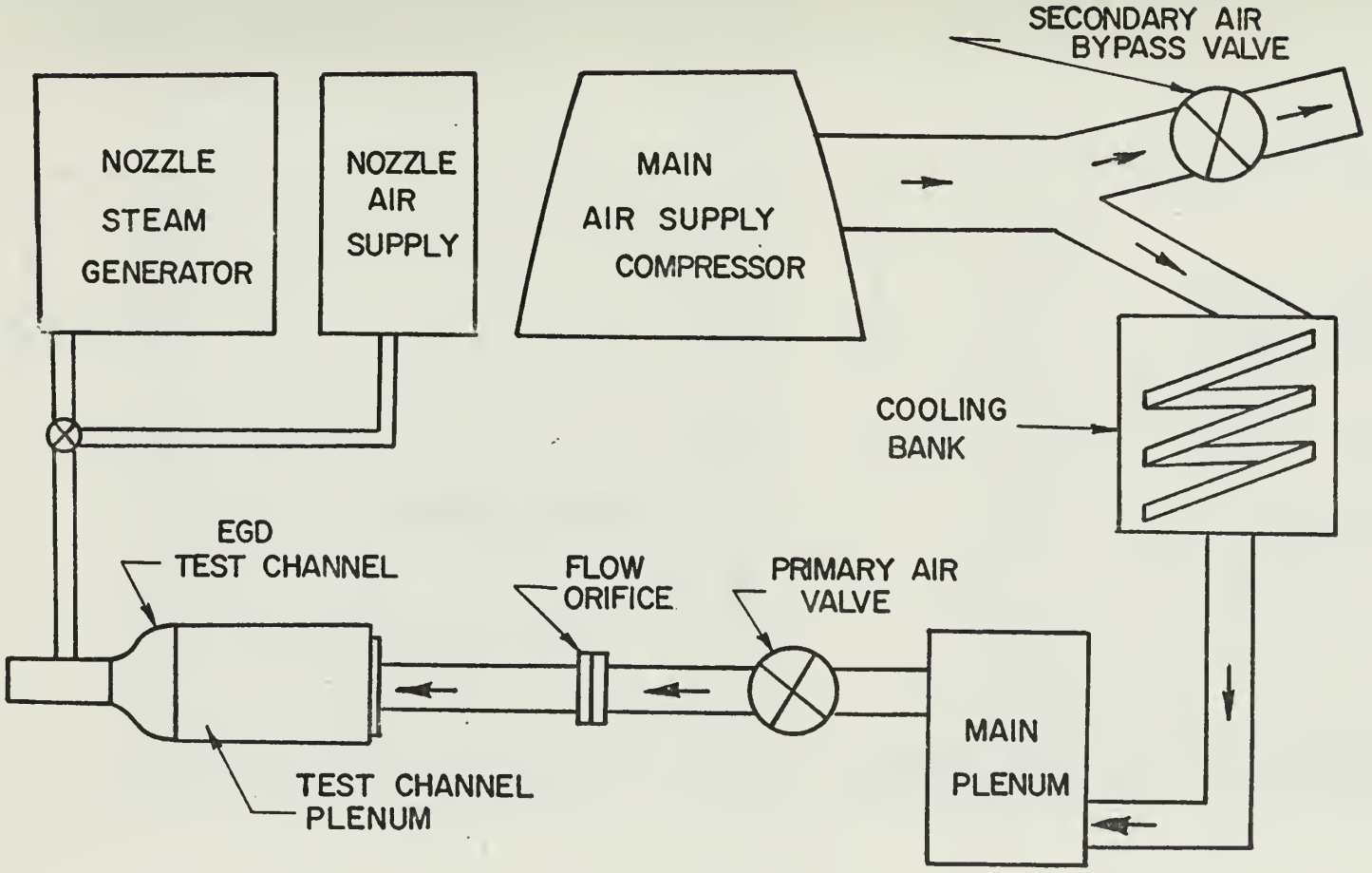

FIGURE 8

AIR AND STEAM FLOW SCHEMATIC.

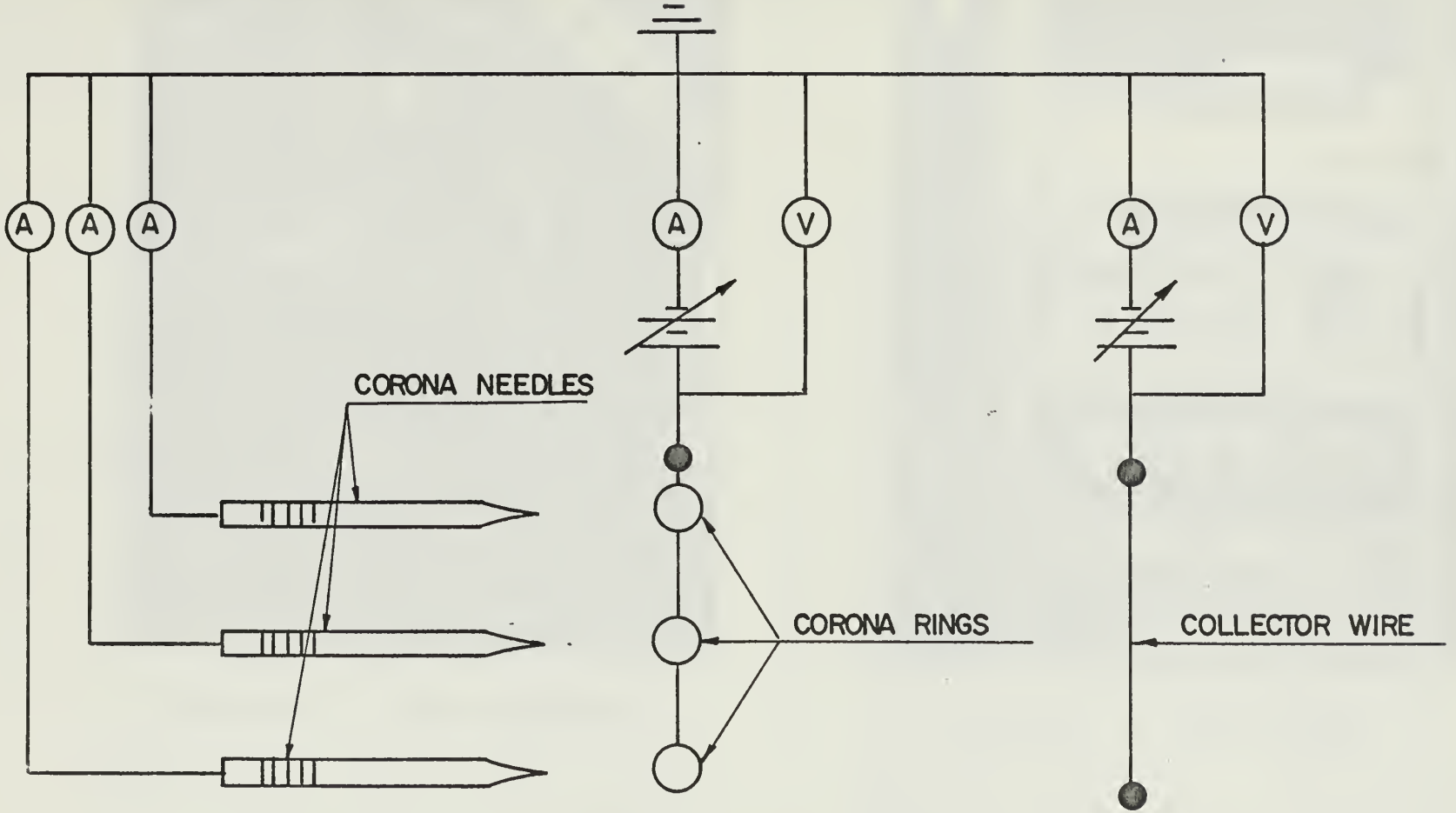

FIGURE 9. ELECTRICAL CIRCUITRY SCHEMATIC

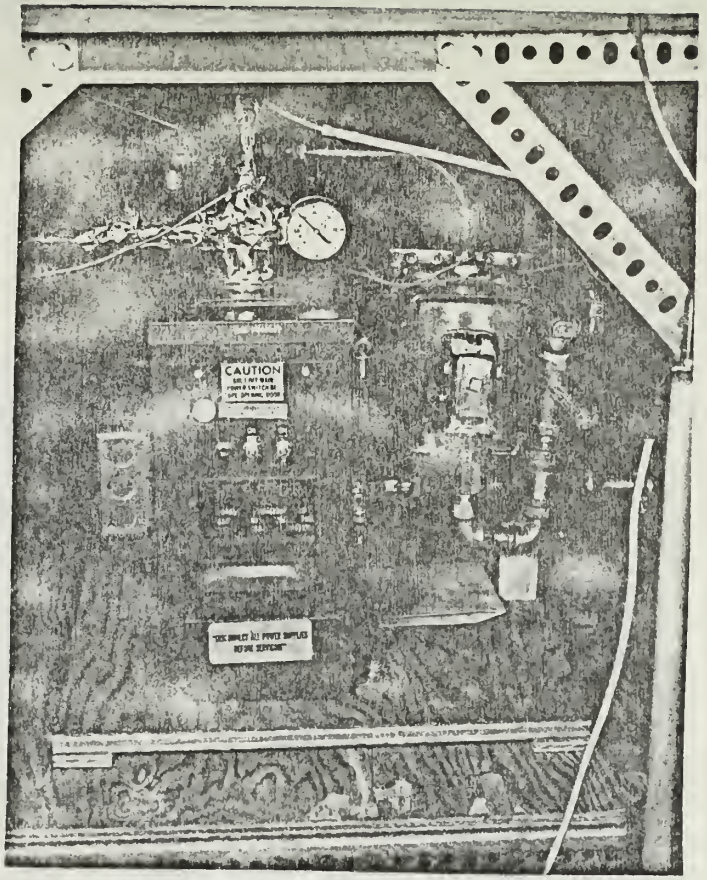

FIGURE 10A STEAM GENERATOR

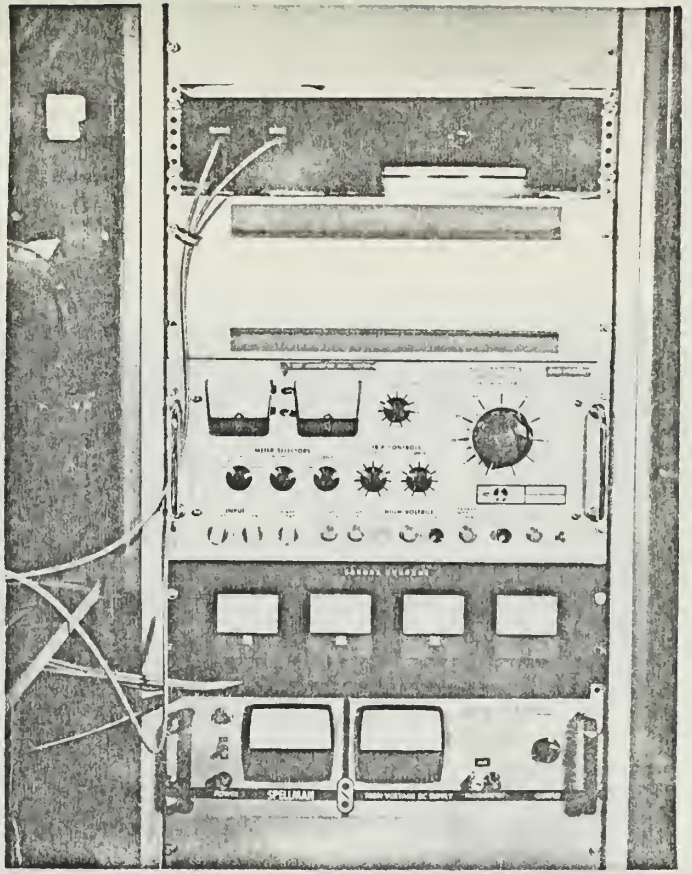

FIGURE 10B POWER SUPPLIES

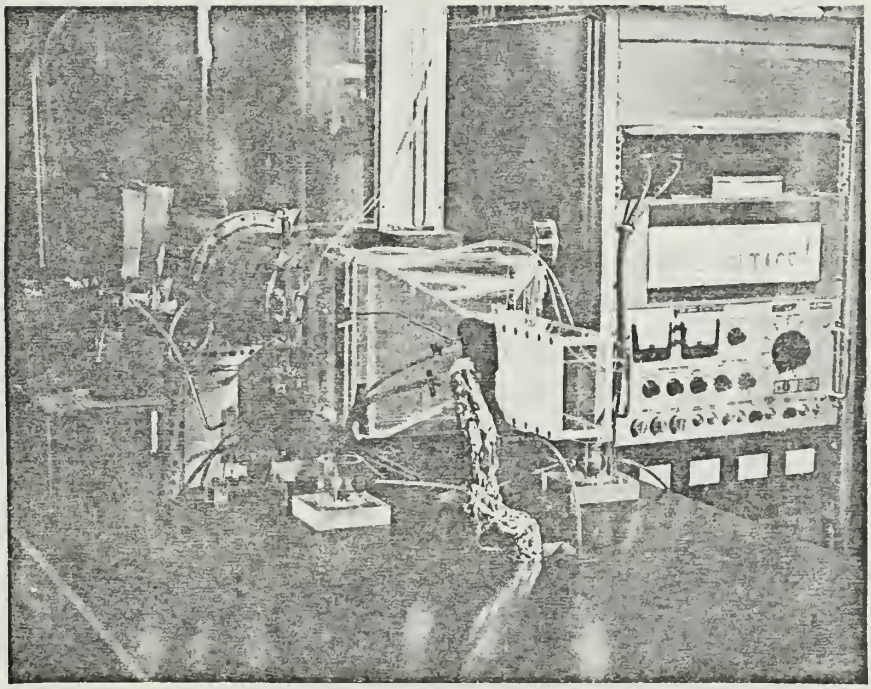

FIGURE 11A SUPPLY AND INSTRUMENTATION LINES

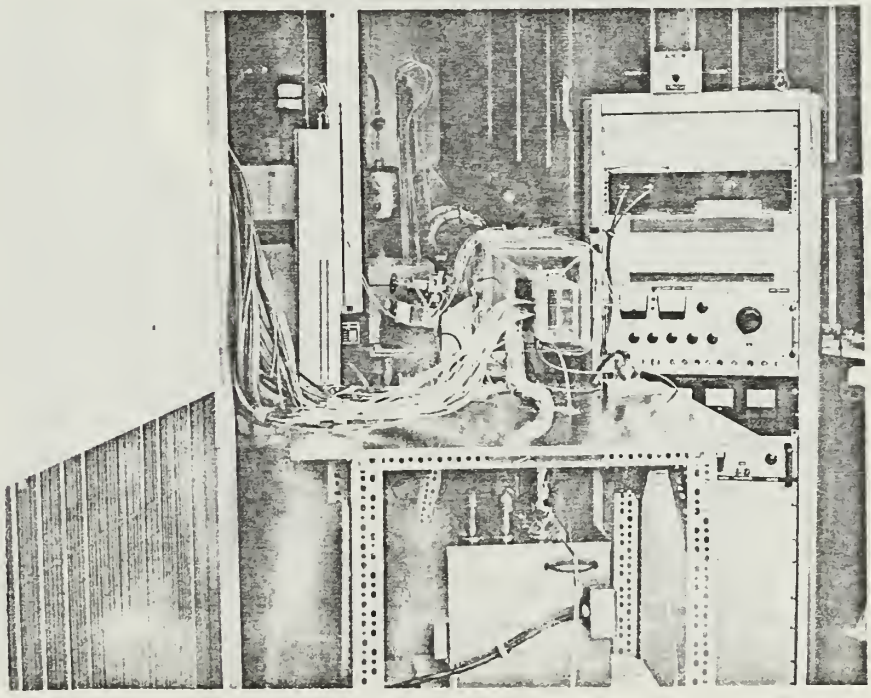

FIGURE 11B EXPERIMENTAL SETUP

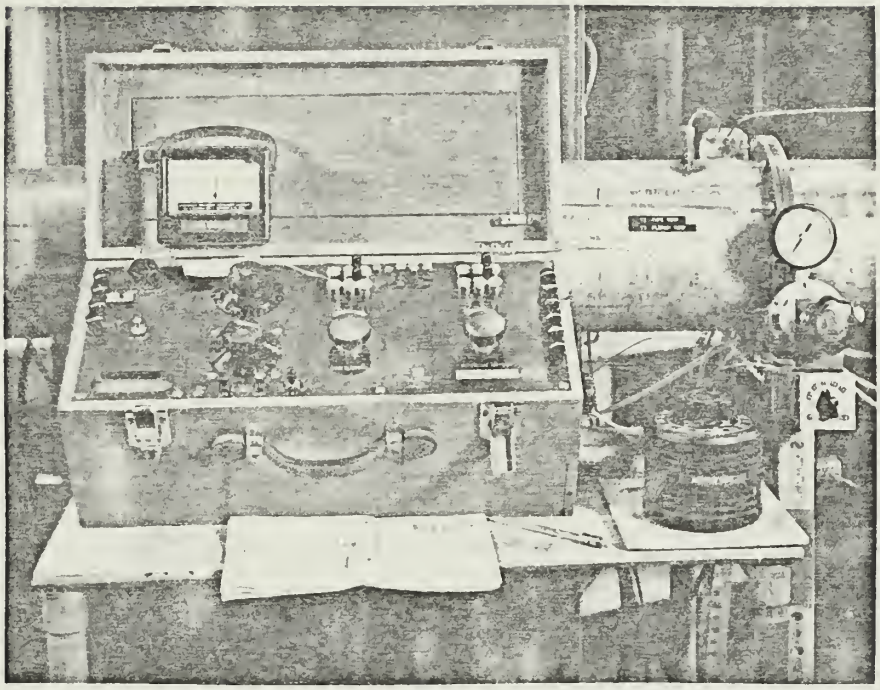

FIGURE 12A TEMPERATURE INSTRUMENTATION

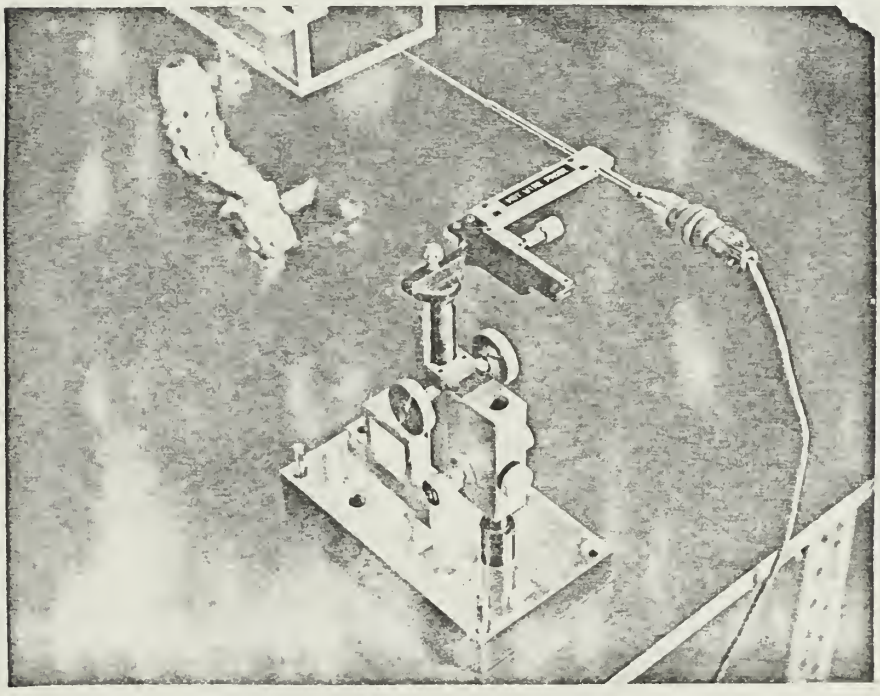

FIGURE 12B HOT WIRE TRAVERSE

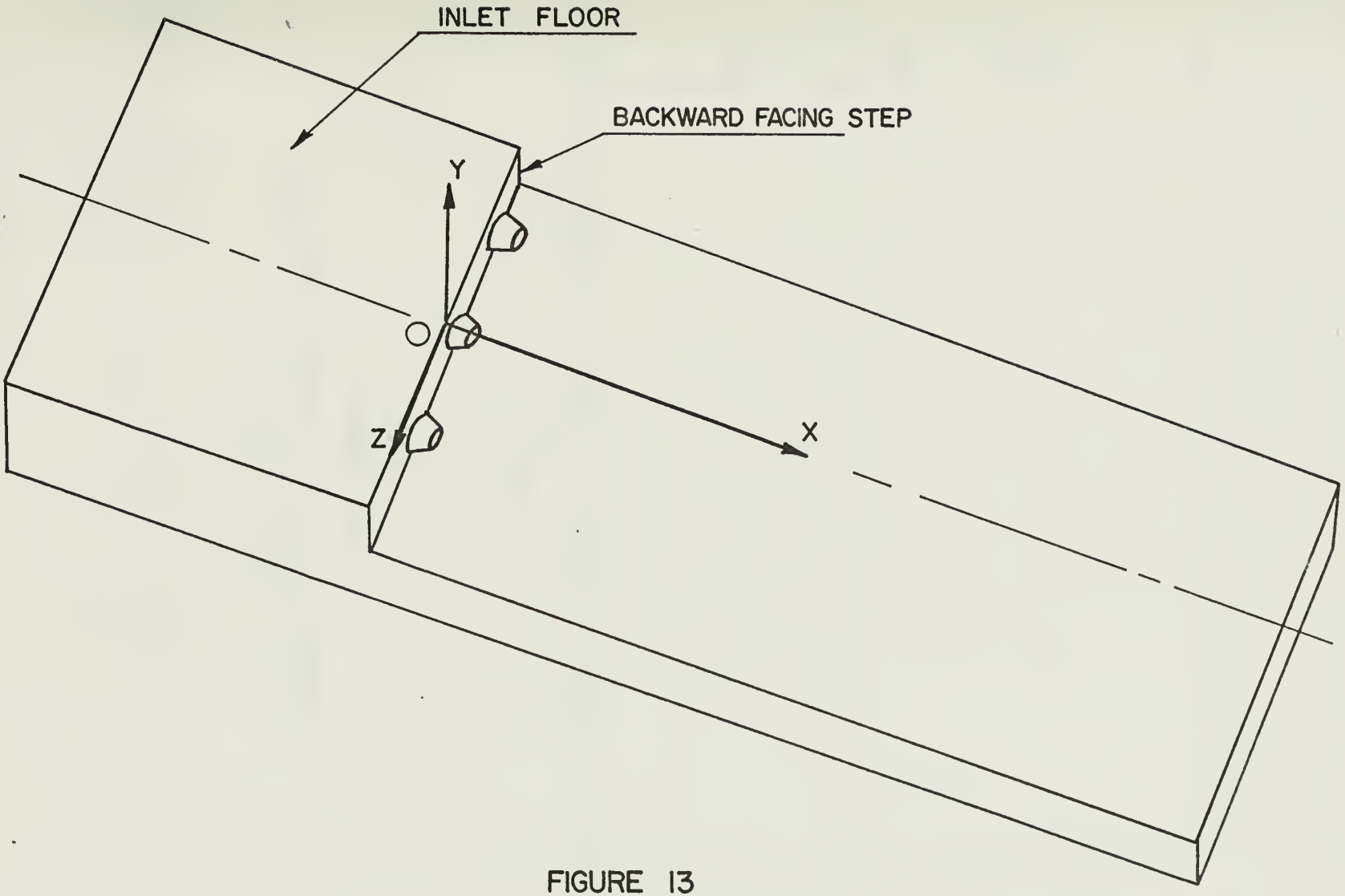

FIGURE 13

COORDINATE SYSTEM ATTACHED TO BACKWARD FACING STEP.

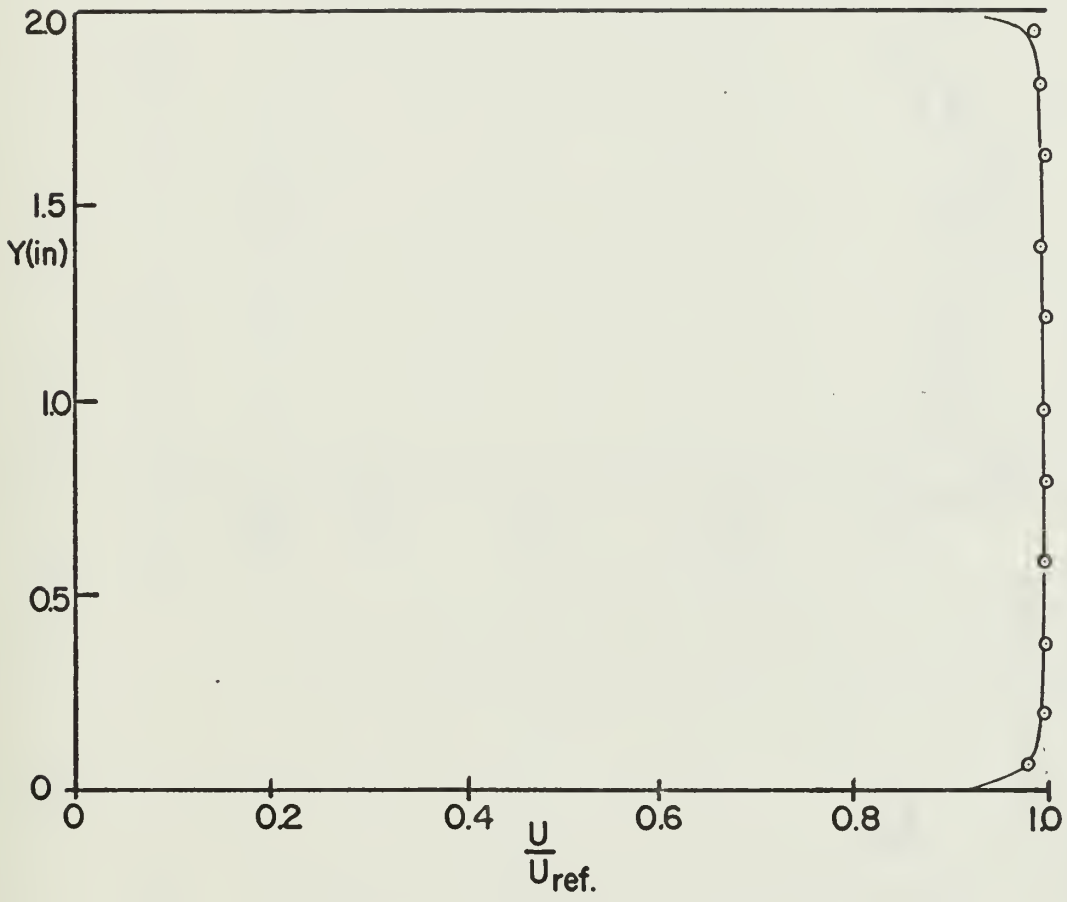

FIGURE 14

VELOCITY PROFILE IN INLET SECTION

X = -1.125 , Z = 0

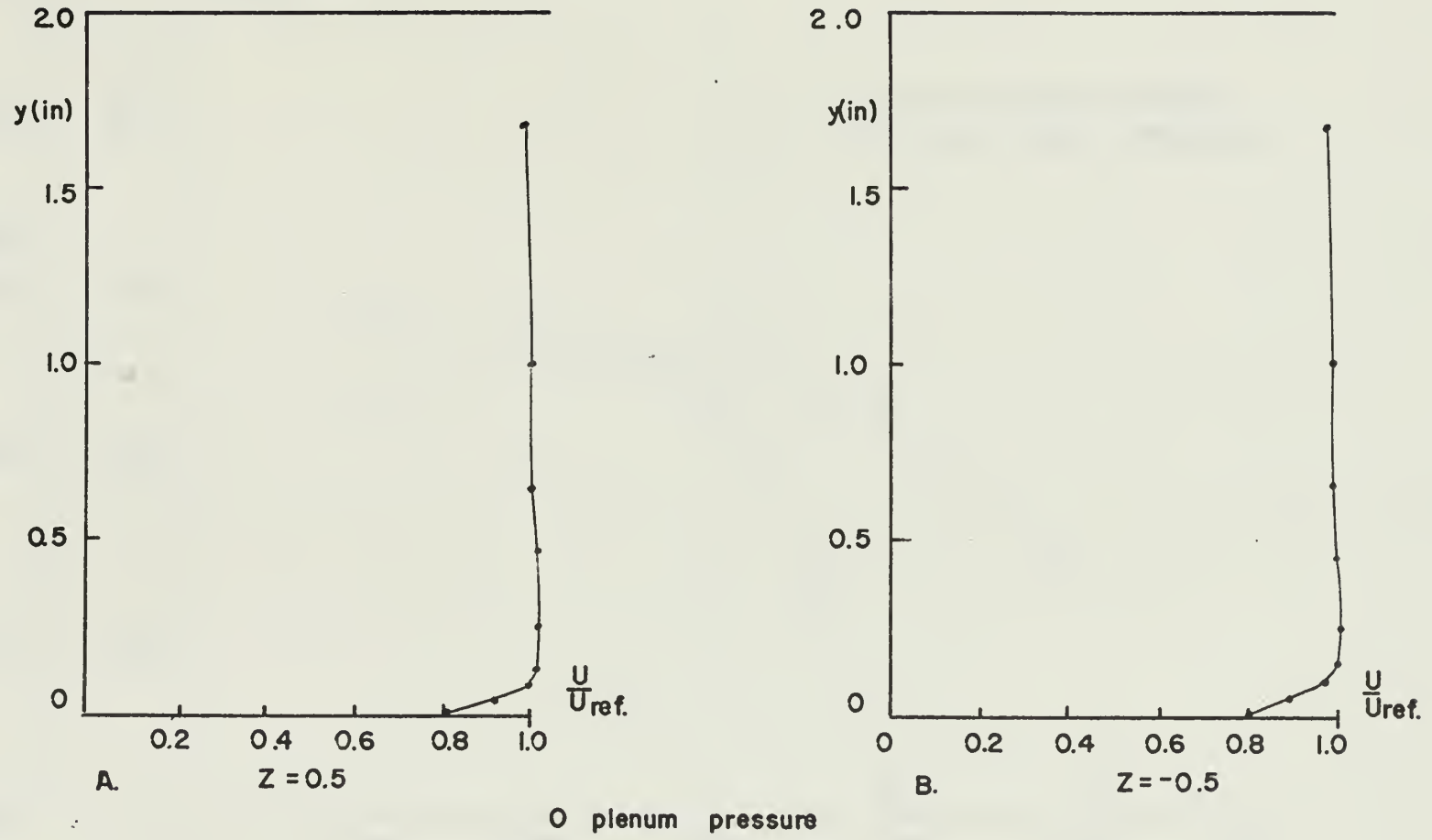

FIGURE 15. VELOCITY PROFILES AT x =0

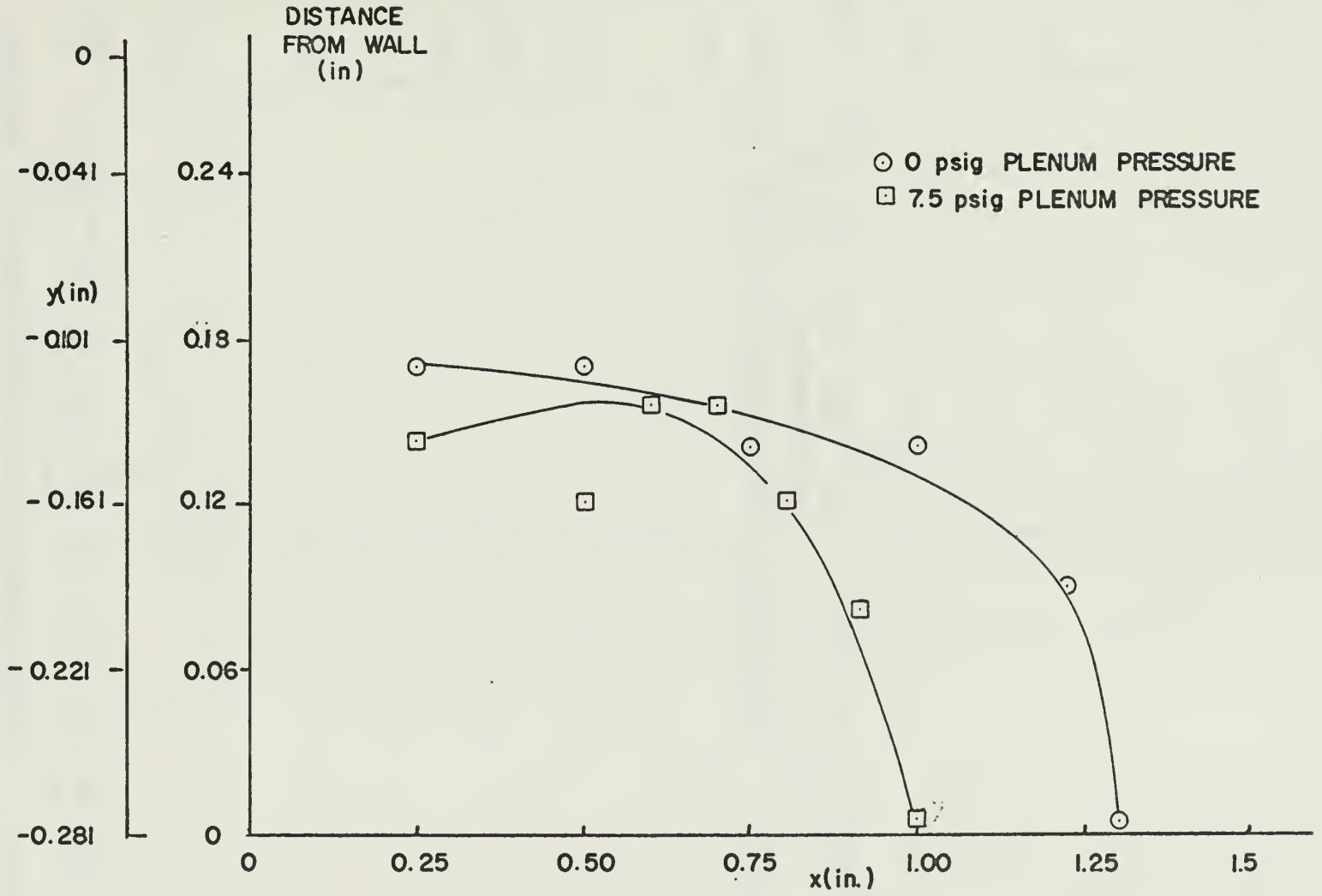

FIGURE 16. POINT OF MINIMUM VELOCITY IN SEPARATED AREA

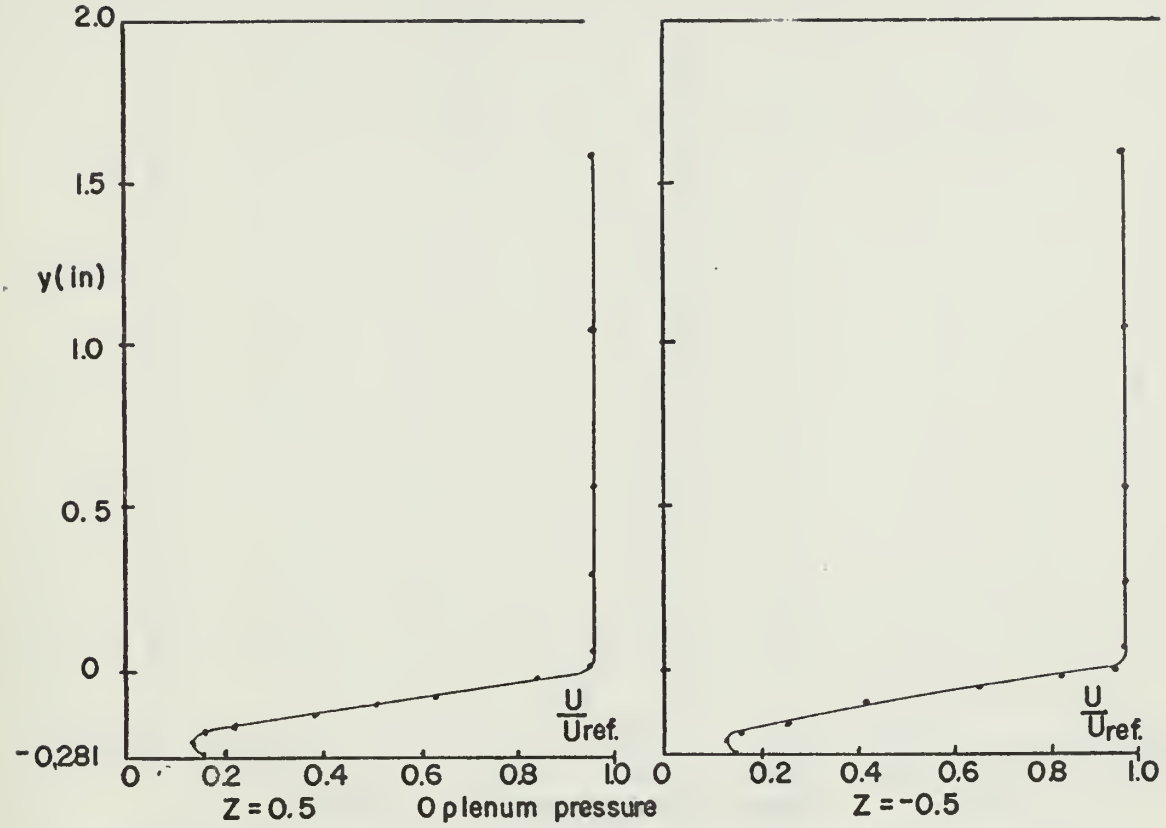

FIGURE 17 VELOCITY PROFILES BEFORE REATTACHMENT x=1.36

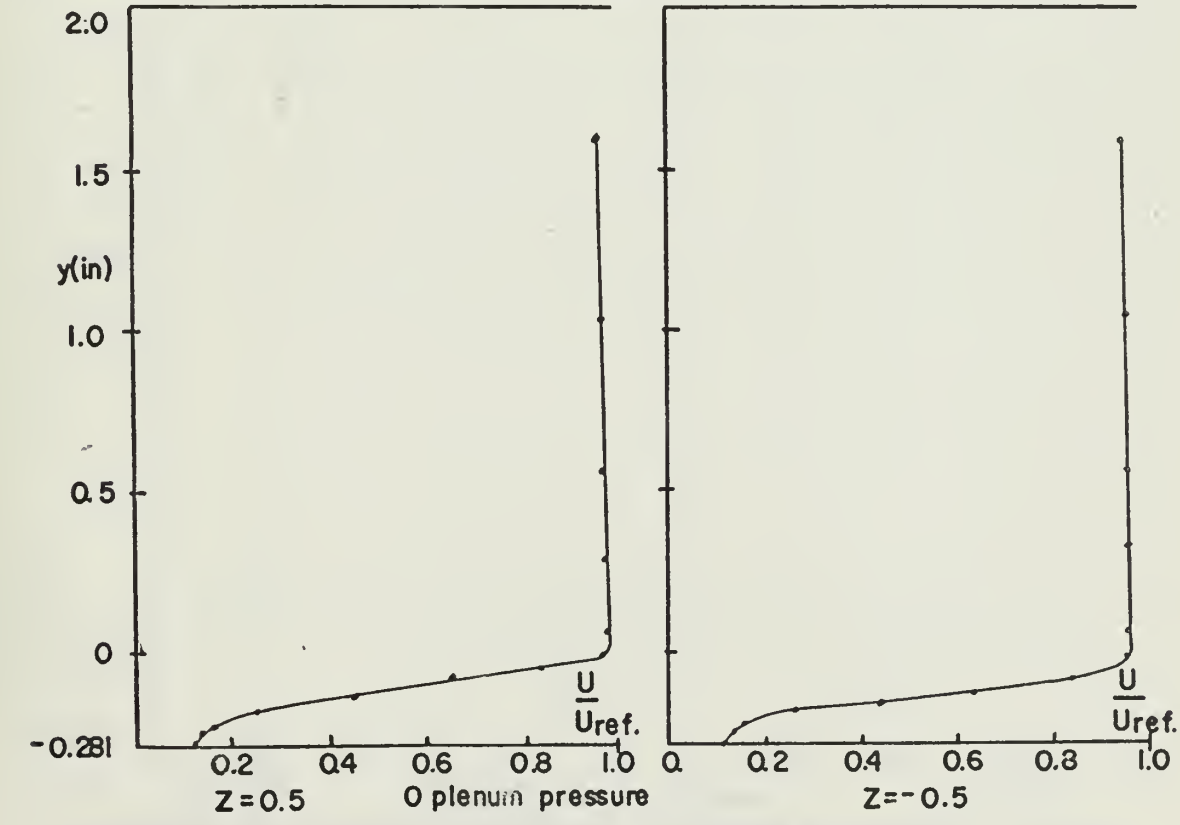

FIGURE 18. VELOCITY PROFILES AFTER REATTACHMENT x = 1.38

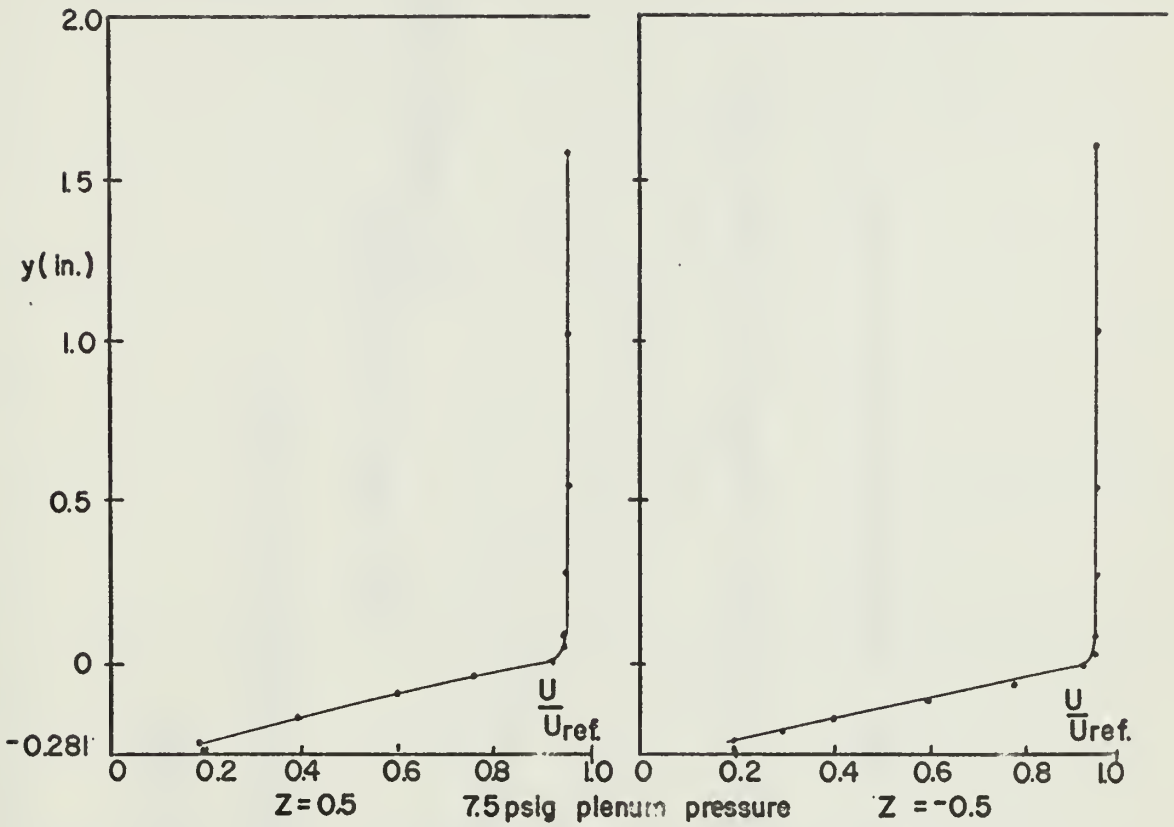

FIGURE 19 VELOCITY PROFILES BEFORE REATTACHMENT x=1.00

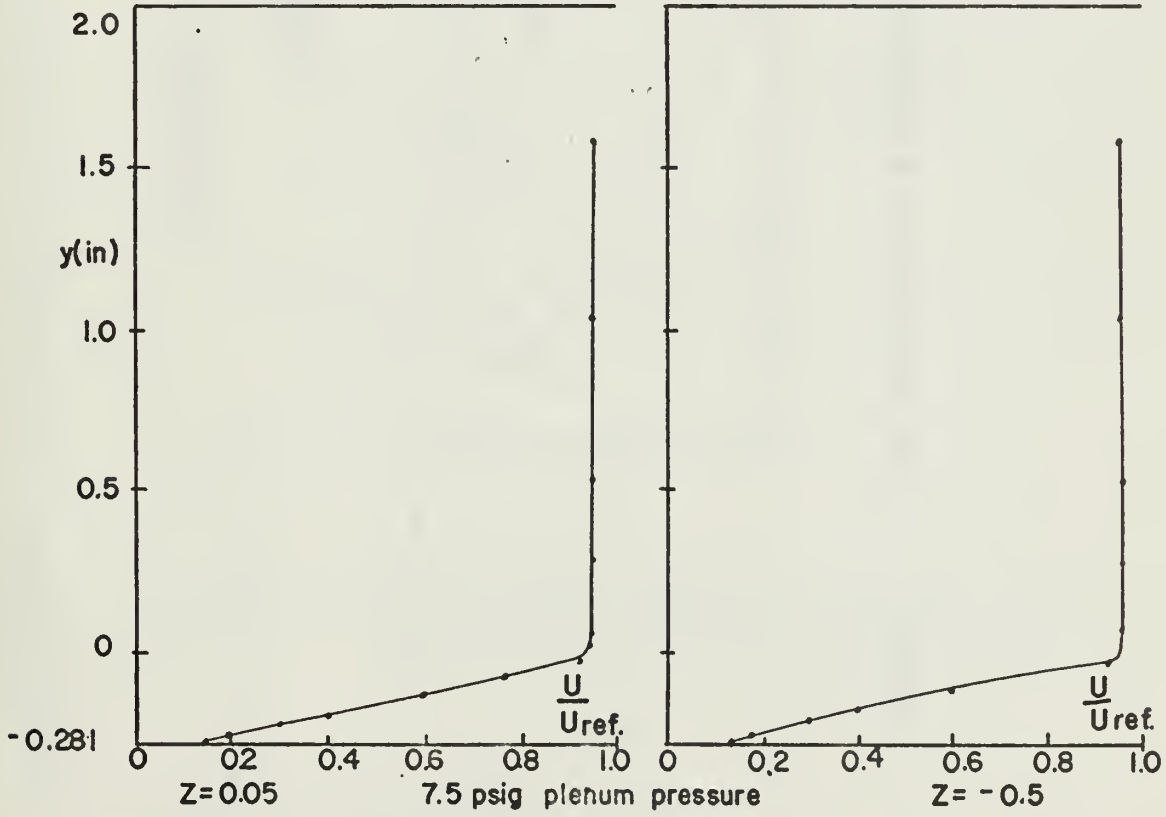

FIGURE 20. VELOCITY PROFILES AFTER REATTACHMENT. x=1.02

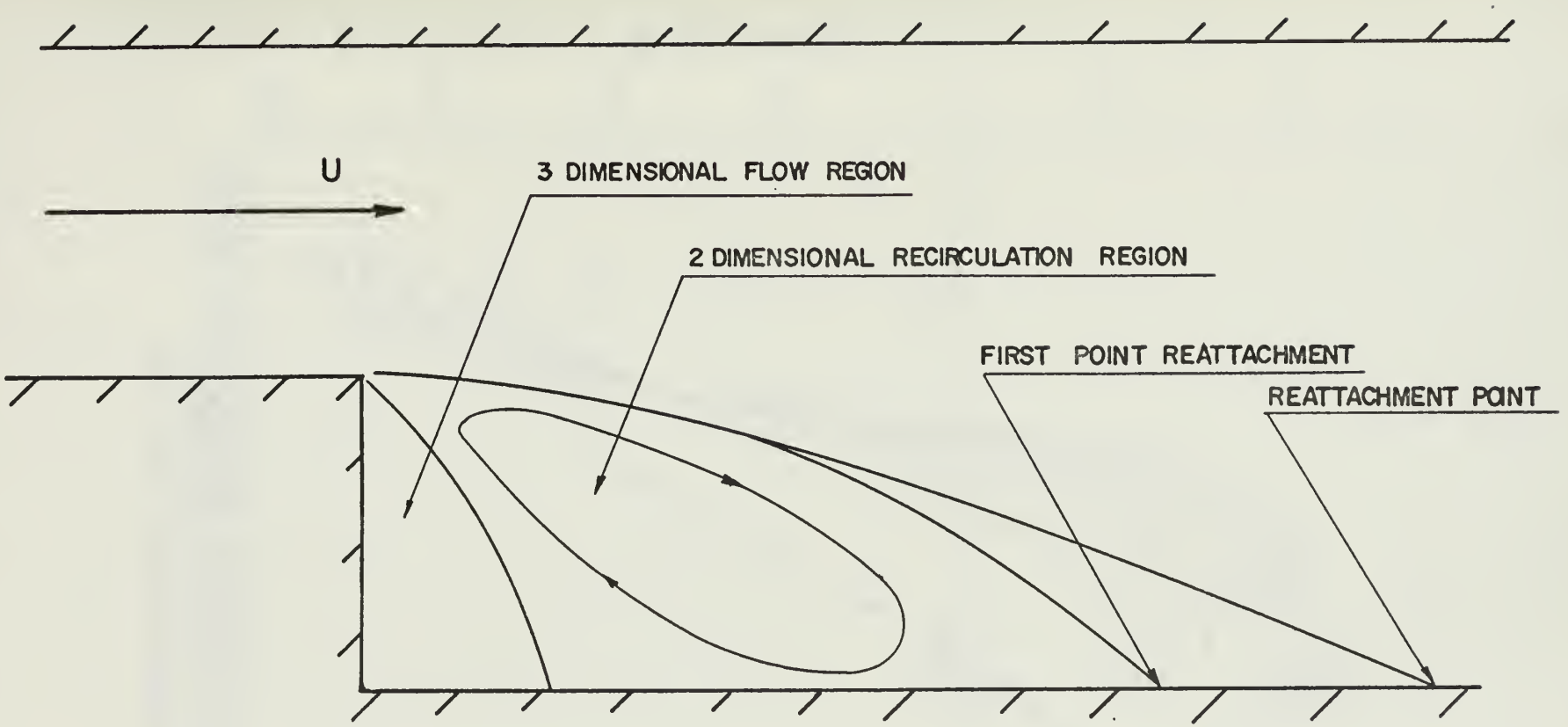

FIGURE 21. FLOW REGIONS IN A SEPARATED AREA DOWNSTREAM FROM A STEP.

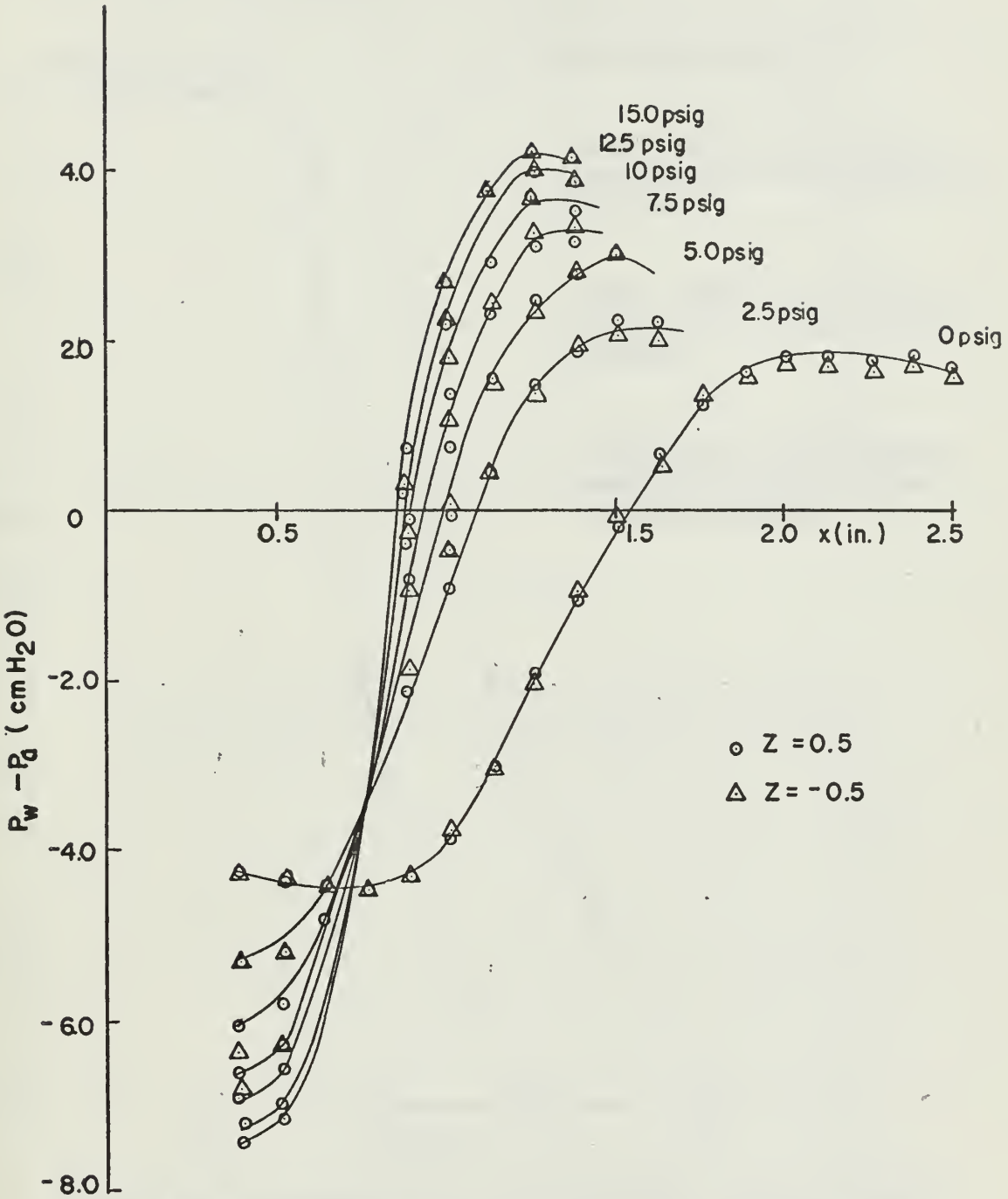

FIGURE 22. PRESSURE PROFILES ALONG WALL IN SEPARATED REGION FOR AIR INJECTION AT THE PLENUM PRESSURES SHOWN.

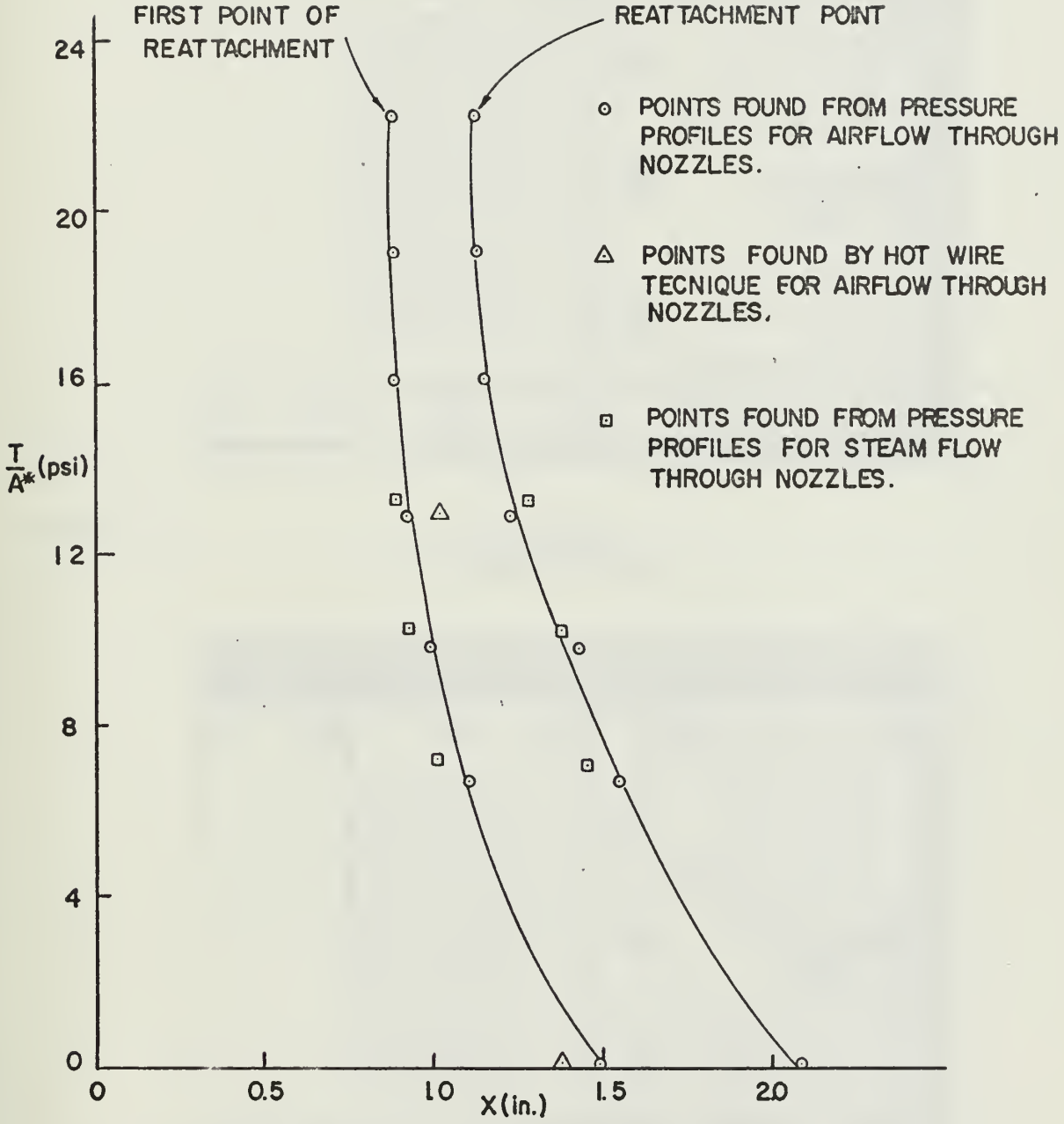

FIGURE 23. MOVEMENT OF REATTACHMENT POINT CAUSED BY NOZZLE THRUST PER UNIT AREA.

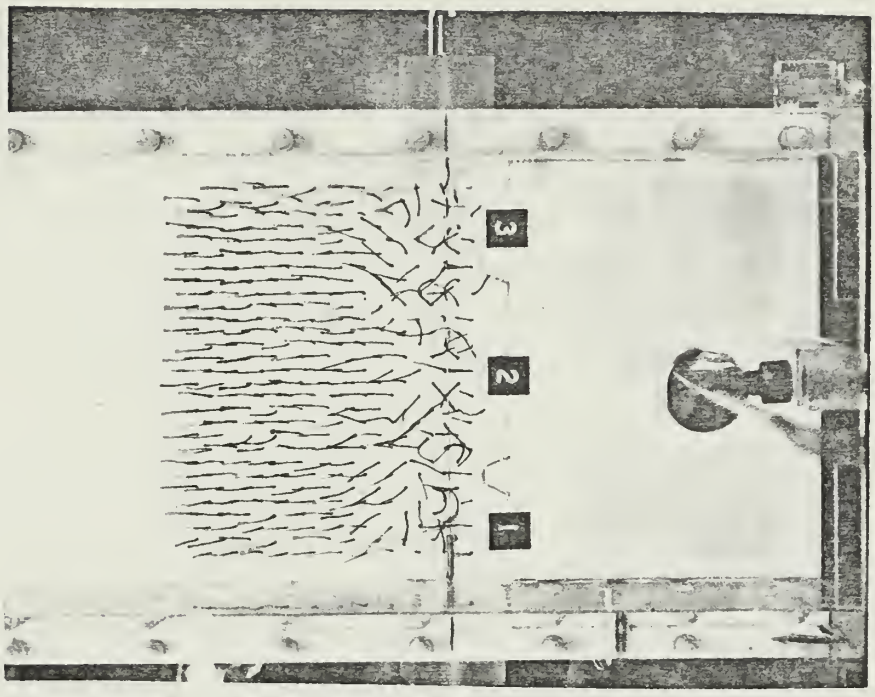

FIGURE 24A

TUFT PATTERN
ZERO PLENUM PRESSURE

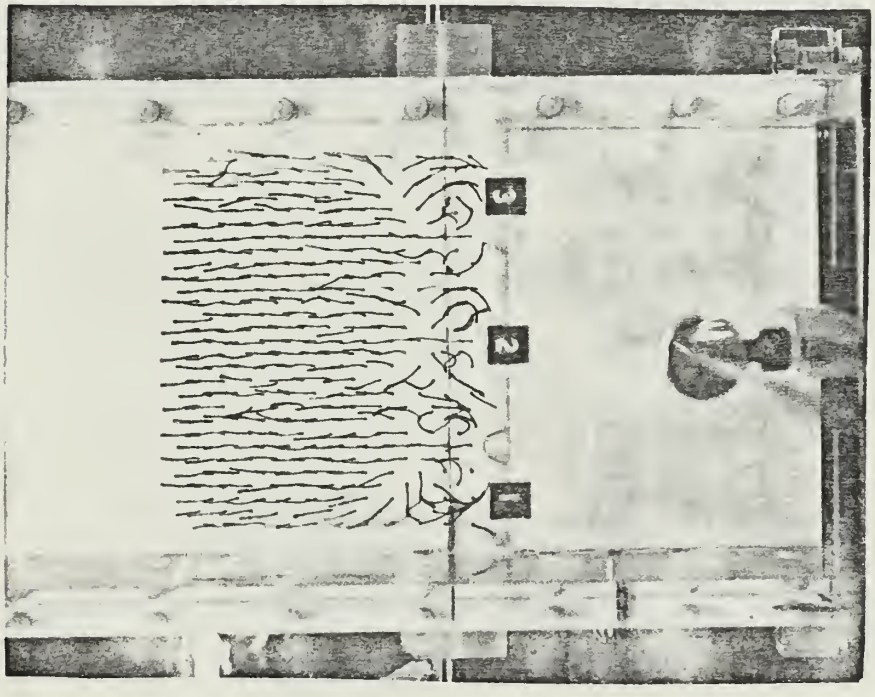

FIGURE 24B

TUFT PATTERN
2.5 psig PLENUM PRESSURE, STEAM

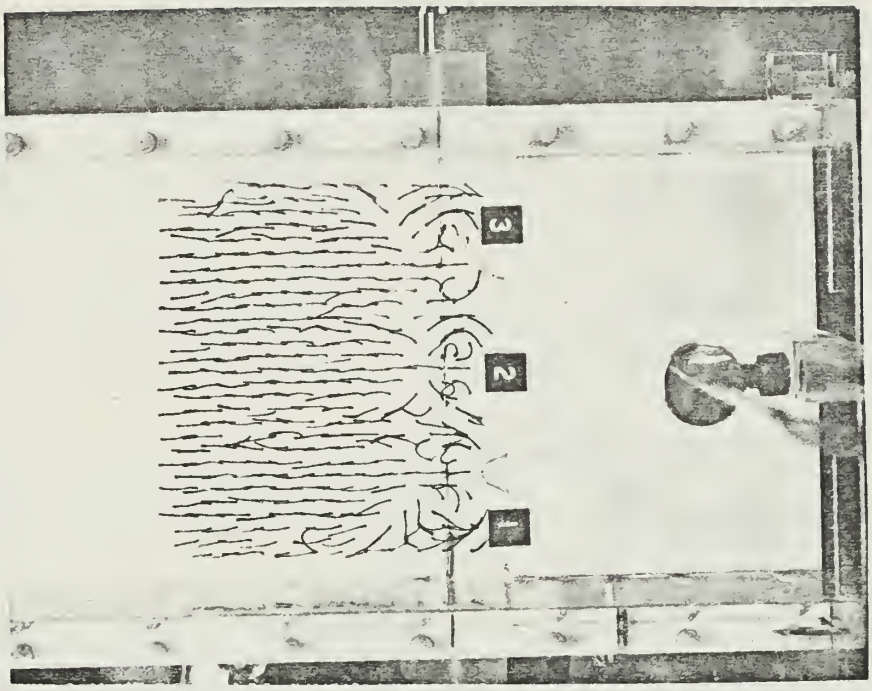

FIGURE 25A TUFT PATTERN
5.0 psig PLENUM PRESSURE, STEAM

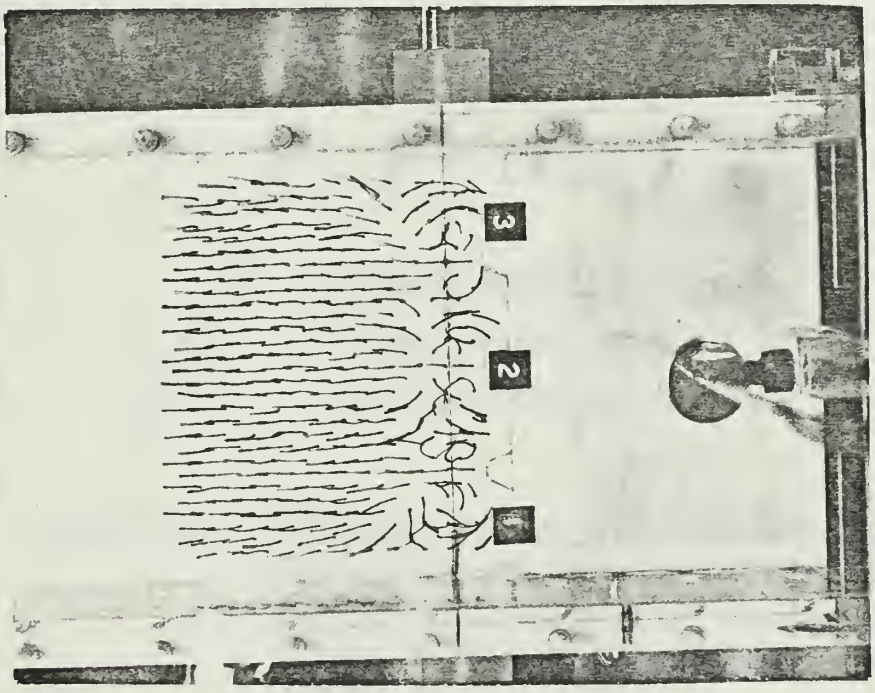

FIGURE 25B TUFT PATTERN
7.5 psig PLENUM PRESSURE, STEAM

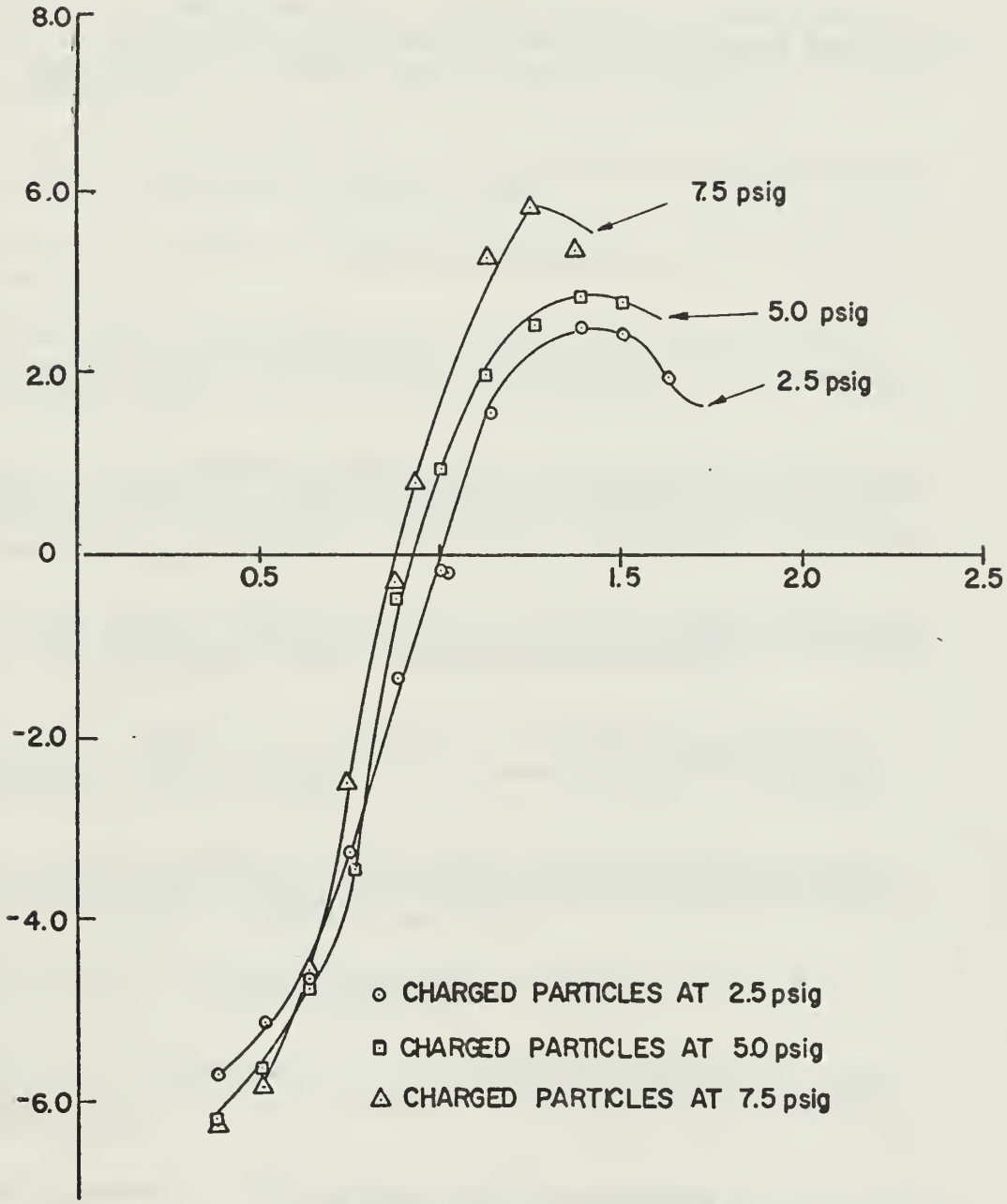

FIGURE 26. PRESSURE PROFILES ALONG WALL IN SEPARATED REGION FOR STEAM INJECTION AT THE PLENUM PRESSURES SHOWN WITH AND WITHOUT CHARGED PARTICLES.

BIBLIOGRAPHY

1. Abbott, D. W. and Kline, S. J., "Experimental Investigation of Subsonic Turbulent Flow over Single and Double Backward Facing Steps", Transactions of the ASME Journal of Basic Engineering, p. 317-325 September 1962.

2. Abbott,I. H. and Von Doenhoff, A. E., The Theory of Wing Sections, Dover Publications Inc., New York 1959.

3. Alston, L. L. (Editor), High Voltage Technology, Oxford University Press 1963.

4. United States Naval Postgraduate School Report NPS-57Z I912A, EHD Research Final Report for the Year 1968-69, by Oscar Biblarz, 30 December 1969.

5. Cheng, Sin-I, Aerospace Applications of Electro-Aerodynamic Interaction, proceedings of the International Symposium on Electrohydrodynamics, Massachusetts Institute of Technology, p. 147-150 31 March, 1-2 April 1969.

6. Aerospace Research Laboratories Report ARL65-4 A Continuation of the Basic Study of Slender Channel Electrogasdynamics, by Bernard Kahn, January 1965.

7. Marks, A., Barreto, E., and Chu, C. K., Charged Aersol Energy Converter, paper presented at AIAA Summer Meeting, Los Angeles, California 17-20 June 1963.

8. Ober, Lt.(j.g.) William, Ion Injector for Single and Two-Phase Electrogasdynamic Generators, Master's Thesis, Naval Postgraduate School, Monterey, California June 1969.

9. Schlichting, H., Boundary Layer Theory, 4th ed., McGraw Hill Book Co. Inc., New York 1960.

10. Shaar, Lcdr. Camille Maleek, Jr., Ionization and Boundary Layer Control, Master's Thesis, Rensselaer Polytechnic Institute, Troy, New York 1947.

11. Shapiro, Ascher H., The Dynamics and Thermodynamics of Compressible Fluid Flow, Vol. 1, p. 102-103, The Ronald Press Co., New York 1953.

12. Stuetzer, Otmar M., Electrohydrodynamic Flow Control, a paper prepared at Sandia Laboratory, Alburquerque, New Mexico (unpublished).

13. Stuetzer, Otmar M., "Instability of Certain Electrohydrodynamic Systems," The Physics of Fluids, Vol. 2, No. 6, p. 642-643, November-December 1959

14. Wood, Karl D., Technical Aerodynamics, 2nd Ed., McGraw Hill Book Co. Inc., New York 1947.

DISTRIBUTION LIST

		No. of Copies
1.	Defense Documentation Center Cameron Station Alexandria, Virginia 22314	2
2.	Library Naval Postgraduate School Monterey, California 93940	2
3.	Commander Naval Air Systems Command Department of the Navy Attn: Dr. H. R. Rosenwasser, Code AIR-310c Washington, D. C. 20360	1
4.	Chairman Department of Aeronautics Naval Postgraduate School Monterey, California 93940	1
5.	Professor T. H. Gawain Department of Aeronautics Naval Postgraduate School Monterey, California 93940	1
6.	Professor K. E. Woehler Physics Department Naval Postgraduate School Monterey, California 93940	1
7.	Professor Oscar Biblarz Department of Aeronautics Naval Postgraduate School Monterey, California 93940	1
8.	Lt. John P. Segen VA 128 NAS Whidbey Island Oak Harbor, Washington 98277	1

Security Classification

DOCUMENT CONTROL DATA - R & D

(Security classification of title, body of abstract and indexing annotation must be entered when the overall report is classified)

1. ORIGINATING ACTIVITY (Corporate author)	2a. REPORT SECURITY CLASSIFICATION
Naval Postgraduate School Monterey, California 93940	Unclassified
	2b. GROUP

3. REPORT TITLE

Electrogasdynamic Control of Separated Flow, A Feasibility Study

4. DESCRIPTIVE NOTES (Type of report and, inclusive dates)

Aeronautical Engineer; June 1970

5. AUTHOR(S) (First name, middle initial, last name)

John Peter Segen

6. REPORT DATE	7a. TOTAL NO. OF PAGES	7b. NO. OF REFS
June 1970	71	14

8a. CONTRACT OR GRANT NO.	9a. ORIGINATOR'S REPORT NUMBER(S)
b. PROJECT NO.	
c.	9b. OTHER REPORT NO(S) (Any other numbers that may be assigned this report)
d.	

10. DISTRIBUTION STATEMENT

This document has been approved for public release and sale; its distribution is unlimited.

11. SUPPLEMENTARY NOTES	12. SPONSORING MILITARY ACTIVITY
	Naval Postgraduate School Monterey, California

13. ABSTRACT

This investigation proposes to determine if electrogasdynamic interactions are feasible for flow separation control. It is shown theoretically that the electric pressure caused by charged particle movement in an electric field produces a pressure increase that is at the lower limit of values needed for flow separation control. The theoretical possibility is also shown using the Navier-Stokes equations with an electric body-force term included.

An experiment is carried out using charged particle injection and acceleration in a separated region beneath a backward-facing step. The experimental results are inconclusive. Recommendations are given to improve the experiment.

DD FORM 1 NOV 65 1473 (PAGE 1)

S/N 0101-807-6811

Security Classification

KEY WORDS	LINK A		LINK B		LINK C	
	ROLE	WT	ROLE	WT	ROLE	WT
Boundary Layer Control						
EGD Flow Control						
Separation Control						
Aerosol Energy Conversion						

Thesis
S4087 Segen
c.1 Electrogasdynamic
control of separated
flow, a feasibility
study.
120117